KANSAS GEOLOGICAL SURVEY
OPEN-FILE REPORT 92-57

THE PETROLOGY AND DEPOSITIONAL ENVIRONMENTS OF THE UPPER PENNSYLVANIAN (MISSOURIAN) LADORE SHALE IN SOUTHEASTERN kANSAS AND ADJACENT OKLAHOMA

by

Peter L. Nimmer

Kansas Geological Survey
1930 Constant Avenue
University of Kansas
Lawrence, KS 66047-3726

ABSTRACT

The Missourian Ladore Shale (Middle Pennsylvanian) overlies the Bethany Falls Limestone and is bounded above by the Mound Valley Limestone on the Cherokee shelf in southeastern Kansas. The Mound Valley pinches out southward, and the Ladore Shale and overlying Galesburg Shale are recognized as portions of the Coffeyville Formation in Oklahoma.

Three Ladore lithofacies are recognized on the Cherokee shelf of southeastern Kansas and northern Oklahoma. The fine-grained, silty-shale lithofacies, present across southeastern Kansas, is dominated by black or grey shale containing fine siltstone interlaminations with abundant plant fragments, and represents rapid deposition of sediments in a low-energy prodeltaic facies. The siltstone-shale lithofacies is predominantly composed of lenticular, wavy and flaser-laminated siltstone interbedded with shale. This lithofacies, which is increasingly thick and more widespread southward in southern Kansas and northern Oklahoma, is extensively bioturbated and contains abundant plant fragments. It represents deposition along a seaward-sloping delta front within a distal bar and distributary mouth bar facies. Shoaling conditions seaward of the river discharge allowed fluvially-deposited sediments to be reworked by tidal activity. The sandstone lithofacies, present only in northern Oklahoma, is composed of very fine-grained massive and laminated sandstone beds that were deposited as distributary channel sand in a lower delta plain setting. Southward increases in grain size and sandstone thickness indicate that Ladore sediments were most likely derived from

the Ouachita Mountains and deposited as a northward prograding fluvial-deltaic complex.

Formation of siderite nodules began before significant compaction. Alteration of potassium feldspars to kaolinite by meteoric waters liberated silica that was precipitated as quartz overgrowths on detritial grains. Poikilitopic calcite cement and pyrite formation occurred as saline waters moved through these units during the deposition of the overlying Mound Valley Limestone. As burial continued, increasing temperatures allowed smectite to be converted to illite. This coupled with maturation of organic matter produced a shale-water solvent which produced framework grain alteration and dissolution in sandstone units. Modern weathering of siltstones and sandstones resulted in increased secondary porosity and production of 'box-work' iron-oxide structures due to dissolution of iron-rich carbonate cements.

TABLE OF CONTENTS

LIST OF TABLES

LIST OF FIGURES

LIST OF PLATES

INTRODUCTION

Geologic setting

During Early Pennsylvanian time, the collision of Laurasia with Gondwana resulted in the formation of two major tectonic provinces in the mid-continent region: the uplifted Ouachita fold belt in southern Oklahoma, and the creation of the Arkoma-Anadarko basin complex, formed by crustal downwarping to the north (Figure 1) (Rascoe and Adler, 1983).

During early Late Pennsylvanian (Missourian) time, the Arkoma basin in southern Oklahoma and the associated Cherokee platform in southern Kansas were the primary depocenters for siliciclastics originating from the Ouachita uplift. Detrital sediments episodically flooded the Arkoma basin, occasionally lapping onto the Cherokee platform, and replacing carbonate production with siliciclastic sedimentation (Watney et al., 1989). The Ladore Shale appears to have formed as the result of deltaic/prodeltaic deposition as deltas prograded across the Arkoma basin and affected the Cherokee shelf during a period of regression (Boardman and Heckel, 1989).

Previous investigations

The Ladore Shale was first described by Adams (1903). Later Hinds and Greene (1915) placed the Ladore in the Kansas City Formation and described this unit as "shale between Hertha and Bethany Falls limestones". Moore (1936) described the type locality of this unit to be at the former town of Ladore (sec 27,

Figure 1: Major tectonic provinces of the mid-continent during Missourian Stage.

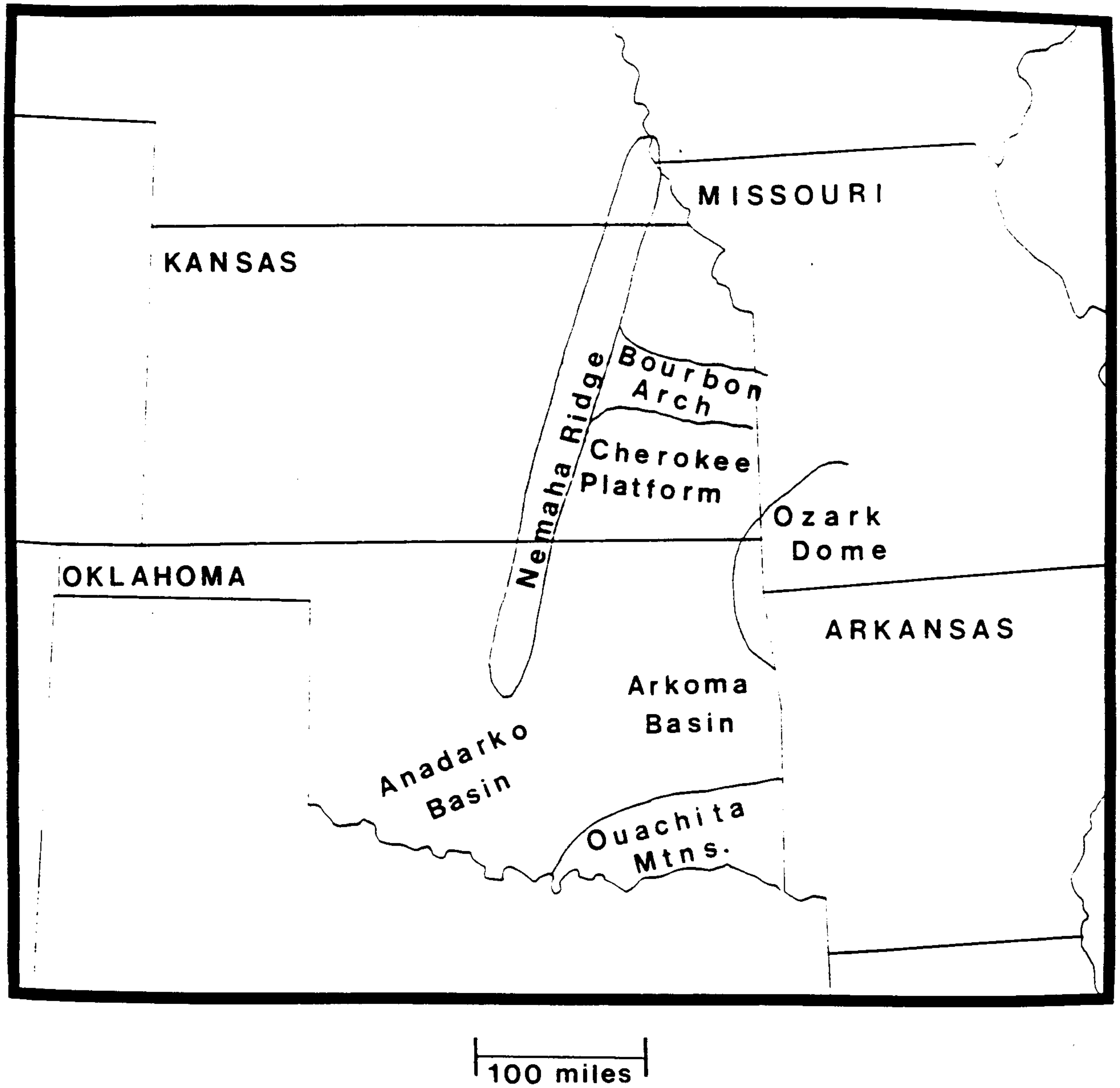
MISSOURI
KANSAS
Nemaha Ridge
Bourbon Arch
Cherokee Platform
Ozark Dome
OKLAHOMA
ARKANSAS
Arkoma Basin
Anadarko Basin
Ouachita Mtns.
100 miles

T 30S, R 19E) in southern Neosho County, Kansas. This unit was further defined by Moore (1936) to include beds between the top of the Hertha and the base of the Swope Limestone.

These units have since been recorrelated, and the bounding units of the type Ladore Shale in southeastern Kansas are now recognized to be the underlying Bethany Falls Limestone Member of the Swope Limestone and the overlying Mound Valley Limestone (Heckel, manuscript in review) (Figure 2).

The informal term "Ladore interval" is used to describe the shaley/sandy interval in about the middle of the Coffeyville Formation of the Kansas-Oklahoma boarder region. In northern Oklahoma the Ladore merges with thick deltaic sediments, and where the Mound Valley Limestone is absent, the sandy intervals of the Ladore and the overlying Galesburg shale are known informally as the "Layton sands" (Watney et. al., 1989). Here the Ladore, also known as the lower Layton sands, is underlain by the black Tacket Shale, a basinal facies, into which the Swope Limestone and older units have graded southward. The Layton sands and associated fine-grained facies are recognizable in the subsurface of northern Oklahoma, and range in thickness from 100 ft (30.5 m) on the Cherokee shelf to 450 ft (137.2 m) in the Arkoma basin (Visher et al., 1980).

Objectives

The objectives of this study were:

1) To interpret the depositional environments and the facies relationships of the sediments within the Ladore interval by examining the lithofacies and sedimentary structures present in cores and outcrops, and to interpret the geometries of Ladore interval lithologies as represented by core and well log

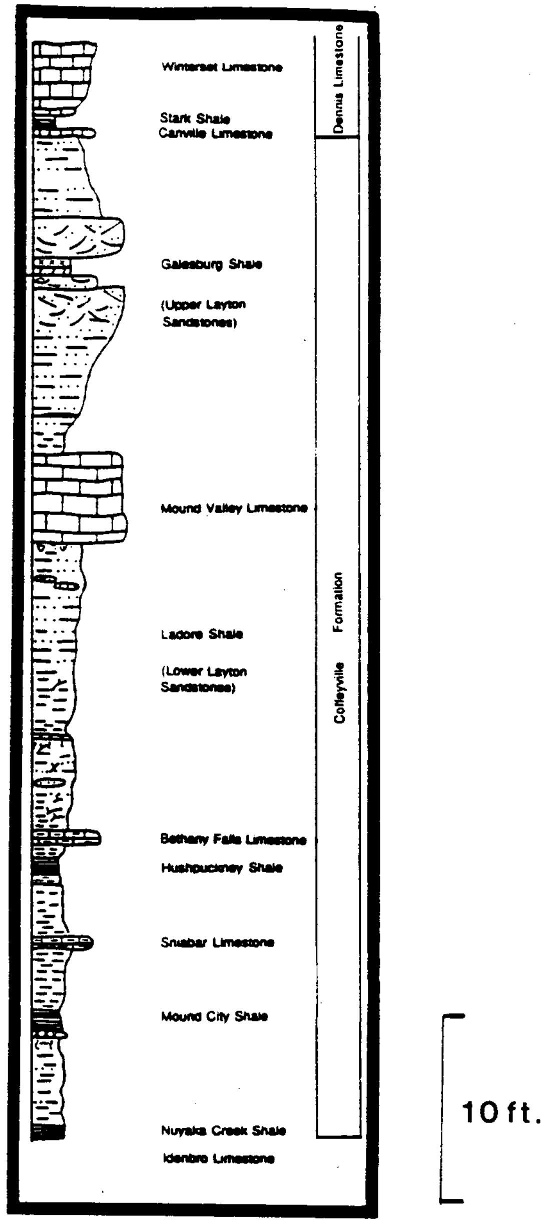

Figure 2: Missourian stratigraphy of southern Kansas, on the lower part of Cherokee shelf showing position of the Ladore Shale in the Coffeyville Formation. Southward towards the Arkoma basin, the Mound Valley Limestone becomes thin or absent, giving rise to upper and lower Coffeyville Formation terminology for the Galesburg and Ladore Shale intervals. Modified from Watney et al, 1989.

data.

2) To determine the extent to which the sandstones and siltstones of this interval have been diagenetically altered, by microscopically examining intergranular cements, and the mineralogy of principal constituents of the sandstone and siltstone layers within the Ladore shale.

3) To interpret the provenance of the siliciclastic material in the Ladore interval.

Methods

Outcrop studies

Fieldwork was undertaken during May and June, 1990, in Kansas and Oklahoma. Eight outcrops of Ladore shale were studied, seven in Kansas and 1 in northeastern Oklahoma (Figure 3). These sections were measured and sketched, and descriptions were made of lithology, sedimentary structures and contacts between lithologies. Sandstone and siltstone beds were sampled for thin-section petrography and S.E.M. analysis. Photographs were taken of characteristic features and structures.

Core data

During May, 1990, eight 2-inch (5 cm) diameter cores from the Kansas Geologic Survey and one similar core from the Oklahoma Geologic Survey were examined (Figure 3). Cores analysis included description of lithologies, sedimentary structures, fossils, cements and types of contacts between units. Representative samples of the sandstones, siltstones and shales were taken for thin-section, S.E.M. and x-ray microanalysis. Photographs were taken of each core, including any diagnostic structures present.

Figure 3: Site location map for the outcrops and cores used in this study.

Cores Sampled:	Location:
1: KGS Dotson	SE/SW Sec.26, T26S, R21E
2: KGS Hines	SW/SW Sec.10, T28S, R19E
3: KGS Heilman	SW/SE Sec.36, T28S, R18E
4: KGS Kinne	SE/NE Sec.13, T28S, R19E
5: KGS Newland	E/NW Sec.6, T30S, R17E
6: KGS Loflin	NW/SW Sec.30, T30S, R17E
7: KGS Gaddy	SE/NE Sec.24, T31S, R16E
8: KGS OLson	NE/NW Sec.30, T31S, R16E
9: OGS Hardin	SW/SW Sec.28, T29N, R15E
Outcrops Sampled:	
A: Page's Pasture	SW/SW Sec.31, T27S, R21E
B; North Erie	NW Sec.20, T28S, R20E
C: South Erie	NW Sec.7, T29S, R20E
D: Parson's Lake	NW/NW Sec.33, T30S, R19E
E: Dixon Mound	SW/SW Sec.27, T32S, R19E
F: Big Hill	NE Sec.18, T32S, R18E
G: Sapulpa Shale Pit	SW/NW Sec. 34, T18N, R11E
H: Lower Coffeyville	NE/SW Sec.14, T20N, R13E

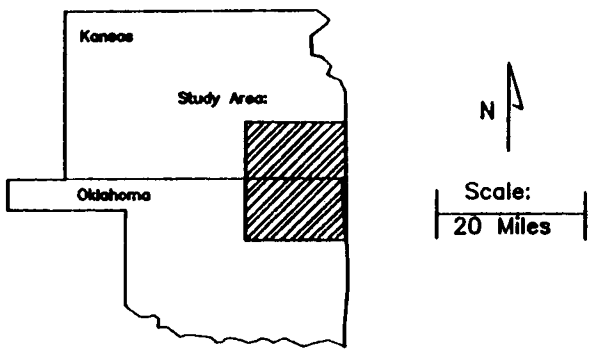

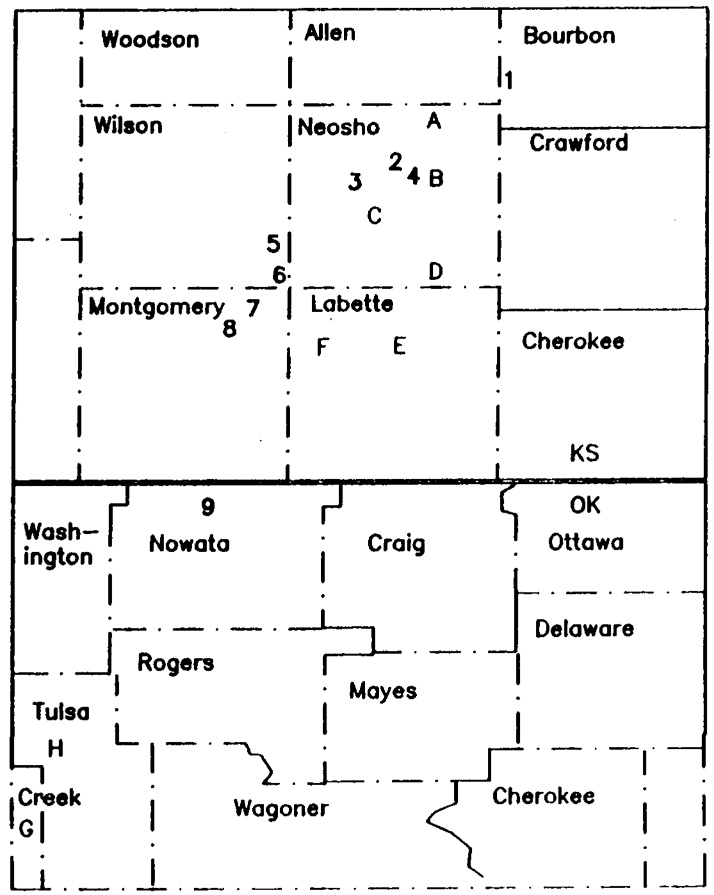

Well log data

Subsurface well logs for Kansas were obtained from the Kansas Geologic Survey, and were analyzed from December to May 1991. More than 100 gamma-ray and neutron density well logs were examined and the thickness and lithologic characteristics of the Ladore shale were noted. In addition, the top and thickness of the Ladore were recorded from 246 previously described Kansas Geologic Survey well logs. Tops and thicknesses were also recorded from 71 well logs from northeastern Oklahoma, which were obtained from the Oklahoma Geologic Survey.

Microscopic analysis

A total of 54 thin sections were made from samples obtained from cores and outcrops. Before being thin-sectioned, each sample was impregnated with blue-dyed polyester resin to prevent plucking and to allow original porosity to be determined more accurately. Selected samples were stained for iron carbonate using potassium ferricyanide and alizarin red-S (Lindholm and Finkleman, 1971). Thirty-two thin sections were examined and point counted. A petrographic microscope was used to determine grain and cement mineralogy, texture, sorting, and diagenesis. Two hundred fifty points were counted on each thin section.

Selected samples were also examined using Scanning Electron Microscopy in order to determine the three-dimensional morphologies of grains, pores, overgrowths and crystal forms of particles below the resolution of the petrographic microscope. S.E.M. samples were trimmed into 10 mm cubes, fractured and mounted on aluminum stubs. A layer of gold-palladium was sputter-coated on the samples to prevent charging. Specimens were examined using secondary electron images at an acceleration voltage between 5 and 15 Kv. Energy dispersive x-ray microanalysis was used in conjunction with the S.E.M for some samples to facilitate mineral identification.

STRATIGRAPHIC OVERVIEW AND LITHOFACIES DESCRIPTIONS

Areal distribution

The Ladore Shale extends from south-central Kansas through southeastern Kansas and into northeastern Oklahoma. It is exposed along the northeast-trending Pennslyvanian outcrop belt of eastern Kansas and Oklahoma. In the subsurface the Ladore varies greatly in thickness, ranging from less than 2 feet (.6 m) in central Kansas and reaching a maximum of 110 feet (33.5 m) in southeastern Kansas (Plate 1).

Stratigraphic overview of the study area

The alternating sequence of thin limestone and siliciclastic units in the Pennsylvanian of the mid-continent region have been interpreted to have been formed in response to eustatic transgressive/regressive sea-level fluctuations (Heckel, 1980). The detrital sandstone and siltstone portions of these cyclothems are thought to be the result of terrestrial material that prograded basinward during regressive events (Heckel, 1977). The Ladore Shale overlies the Bethany Falls Limestone (a regressive limestone at the top of the Swope cycle in eastern Kansas) and underlies the Mound Valley Limestone (a minor transgressive-regressive cycle of marine inundation) in southeastern Kansas (Heckel, manuscript in review). The Mound Valley has been traced through eastern Kansas into northeastern Oklahoma where it lies near the middle of the

Coffeyville Formation. The Ladore Shale has been interpreted to have been deposited during a lowstand in the late regressive phase of the Swope sequence (Boardman and Heckel, 1989).

The sediments within the Ladore Shale vary in thickness and composition across the Cherokee shelf region. In the Bourbon County area of eastern Kansas, the Ladore is a thin, calcareous shale abruptly overlying the Bethany Falls Limestone. The Ladore thickens southward into southern Neosho County, where, near its type area it is represented by a thick gray shale with thin sandstone beds, including a coal and underclay. Southward in central Labette County, the Ladore interval is about 60 feet (18.3 m) thick, and consists predominantly of shale that contains zones of marine fossils and plant fragments. In the Coffeyville area, the Ladore becomes increasingly sandy and contains many thick sandstone beds, each of which coarsen upwards from a thick silty shale to a fine-grained sandstone. On the lower part of the Cherokee shelf, where the Mound Valley limestone pinches out, the Ladore is directly overlain by the Galesburg Shale.

Lithofacies descriptions

The Ladore Shale can be subdivided into three major lithofacies based on amount of shale present and dominant sedimentary structures. These lithofaces are 1)silty-clay shale, 2) interbedded siltstone and shale, and 3) quartz sandstone. The characteristics of these lithofacies are summarized in Table 1.

Table 1: Sedimentary structures present in the three lithofacies of the Ladore shale. a = absent, r = rare, o = occasional, c = common.

[redacted]

Lithofacies:	Sedimentary Structures								
	lam. shale	*siltstone interbeds*	*wavy/lent. laminations*	*small x-lamellae*	*large x-beds*	*plant fragments*	*burrows*	*siderite nodules*	*fossils frags.*
Silty-clay shale lithofacies	c	a - r	a	a	a	c	c	c	a - o
micrite layers	a	a	a	a	a	a	a	a	o
skeletal grain layers	a	a	a	a	a	a	a	a	c
quartz siltstone layers	r - o	c	a - r	a - r	a	a - r	o	a	r - o
Siltstone-shale lithofacies	c	c	c	o - c	a	c	a - o	a - o	a - r
mixed siltstone-shale fabric	o	c	c	a - o	a	o	o	a	r - o
fine-grained sandstone fabric	a	c	c	a - c	a	o	o	a	r - o
Sandstone lithofacies	a - r	o	r - c	c	c	o	a	a - r	a

Silty-clay shale lithofacies

Core observations

The clay shale lithofacies comprises a fissile silty clay shale, which varies in color from black to gray (See appendix A for core descriptions). Fine siltstone interlaminations are occasionally present as isolated layers and may be calcareous. Small bivalves, crinoid fragments and other abraded skeletal fragments are common. Burrows are common and may be filled with carbonate-cemented siltstone. Brown oxidization halos often surround burrows and other organic material. Plant fragments are ubiquitous in this facies and range in size from less than one inch (2.5 cm) up to the entire width of the core (2.5 inches, 0.06 m). Tan nodules, identified as siderite based on EDX analysis, are also present in some cores, particularly in samples from the Hardin, Olson and Gaddy cores (Figure 4).

The most common sedimentary structures are fine laminations or homogeneous bedding but include some layers of starved ripples composed of fine-grained siltstone. In some core samples, lamellae are brown-colored, in contrast to the dominant gray-black color of most of the shale in this lithofacies. These thin intervals of brown shale (<5 cm thick) are roughly parallel to the lamellae of the shale, which are not disrupted by these color variations (Figure 4).

Outcrop observations

In outcrop, the thin shale laminations of this facies are especially apparent as millimeter-scale partings. Thin, laterally persistent siltstones and carbonate beds generally less than 2 inches (0.05 m) occur at the Dixon Mound, Parsons Lake, Lower Coffeyville and Sapulpa Shale Pit localities (see appendix A for outcrop

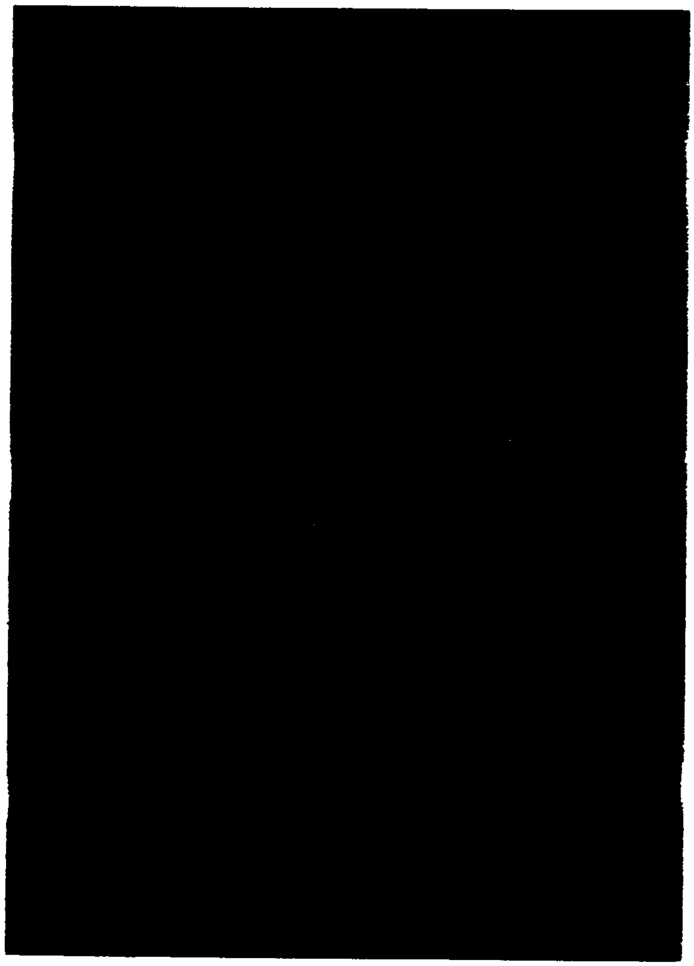

Figure 4: Tan siderite nodules (N) and brown shale in the silty-clay shale lithofacies. Note that bedding is disrupted by siderite nodules, but not by brown shale lamellae (arrows). Olson core, 330' 0".

descriptions). These layers are carbonate cemented, quartz rich and many show sharp upper and lower surfaces (Figure 5). Some of these layers are burrowed or contain shale laminations. Thin, fine-grained sandstone beds with similar characteristics are also present in this lithofacies, but in lesser amounts.

Plant fragments were observed at most outcrops, with large fragments up to 8 inches (0.2 m) present in great abundance at the Big Hill section (Figure 6). A six inch (0.15 m) thick coal with a poorly developed gray mudstone underclay were observed at Parsons Lake. The presence of at least one additional coal bed at this section has been reported.

The silty clay shale lithofacies of the Ladore Shale frequently shows a sudden color change just below the contact with the overlying Mound Valley Limestone, becoming mottled orange-yellow in color. Bedding surfaces and laminated black shale decrease in abundance towards the top of the Ladore, where massive bedding and black shale chips dominate. These variations were found at Big Hill Ladore, Parsons Lake, Dixon Mound, and North Erie sections. This color and texture change is assumed to be the result of modern soil formation processes.

Nodular concretions of siderite are common in most outcrops often in great abundance along some horizons, notably Parsons Lake, Lower Coffeyville, North and South Erie and Sapulpa Shale Pit outcrops. These oblate-disc shaped features are frequently less than 6 inches (0.15 m) in diameter. The long axes of concretions are generally parallel to bedding.

Microscopic analysis

The fissile nature of the shale in this lithofacies caused thin-section preparation to be difficult, although thin-sections of the laterally persistent siltstone and

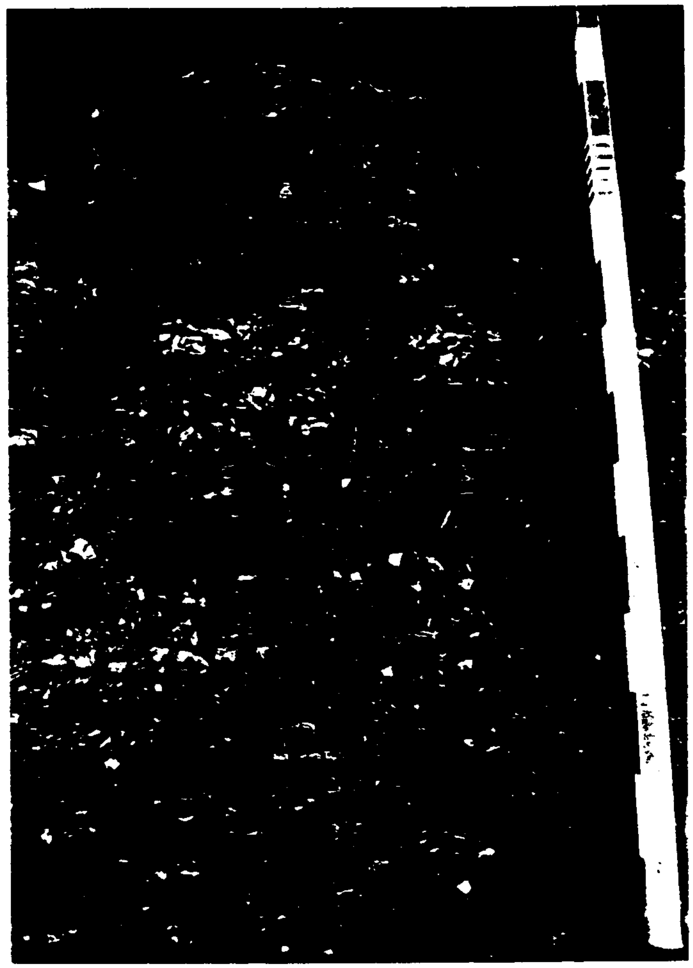

Figure 5: Carbonate-cemented quartz siltstone beds with sharp upper and lower boundaries.10 cm divisions of Jacob staff. Parsons Lake section. 2.0 feet above water level.

Figure 6: Large plant fragment near top of Ladore Shale.
Pen is 17 cm long. Big Hill section.

carbonate lenses were prepared and examined. These beds are rare and less than 2 inches (5.0 cm) thick. These beds represent changes in the depositional history of this lithofacies and will be further discussed in the depositional environments chapter. Microfacies analysis reveal three distinct lithologies of these well indurated layers: micrite (calcilutite), skeletal grains (skeletal calcarenite), and fine-grained, calcite-cemented quartz sandstones and siltstones.

Micrite layers are composed of micrite and microspar with scattered silt-sized quartz grains, which often occur in lenses or layers (Figure 7). Within these thin (< 1 mm) quartz-rich layers, grains range in size from fine-silt to very-fine sand (0.016 mm to 0.07 mm). Silt-sized mica flakes are widely disseminated through the micrite, and are commonly concentrated in layers. Brachiopods, ostracodes, and foram fragments are sparse, and some are pyritized.

The skeletal grain (skeletal calcarenite) layers are composed of partially or entirely recrystalized coarse sand-sized fossil fragments with varying amounts of matrix material composed of micrite and clastic grains. Fossil groups present in these layers include forams, brachiopods, productid spines, crinoids, gastropods, and ostracodes. These fragments have been recrystallized into micrite, neomorphic microspar or blocky spar (Figure 8). Poikilotopic intragranular calcite cement is present between skeletal fragments and clastic grains.

The calcite-cemented fine-grained sandstone to coarse-grained siltstones show quartz grains, muscovite, authigenic kaolinite and illite clays as the major mineral constituents (Figure 9). Other components include micrite, pyrite, organics (including wood fragments), feldspars and calcite as grains or poikilotopic cements. Fossils are rare, although ostracodes may be present in

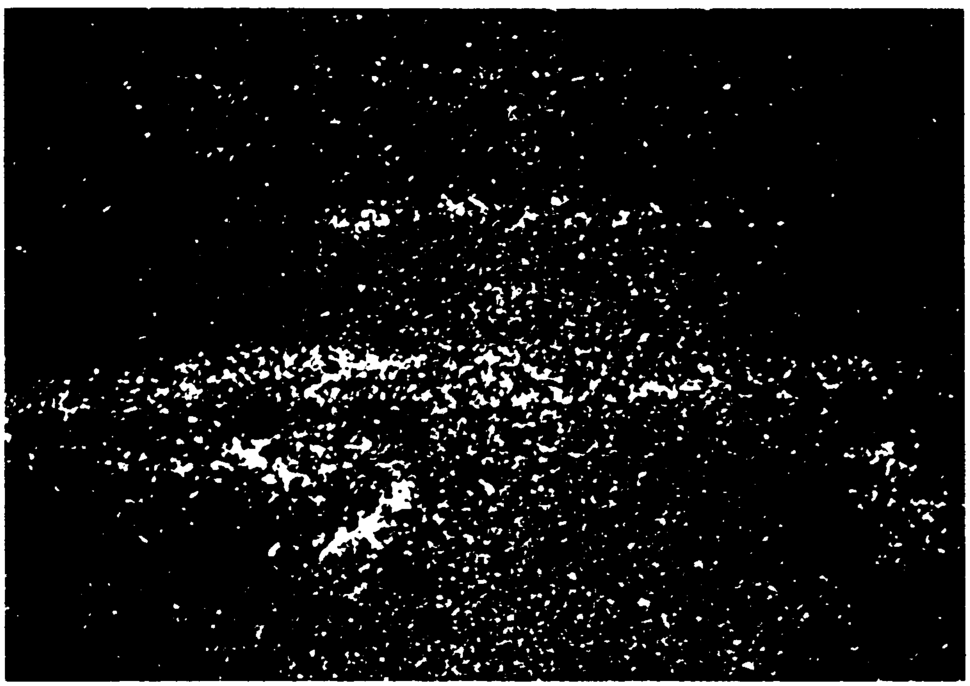

1.7 mm.

Figure 7: Siltstone lamellae (S) in a micrite layer of the silty-clay shale lithofacies. Sapulpa Shale Pit 2.8 s, cross-polarized light.

1.7 mm

Figure 8: Photomicrograph of skeletal calcarenite layer in the silty-shale lithofacies. Note the complete recrystillization of the skeletal fragments. Gaddy 309' 11", plain light.

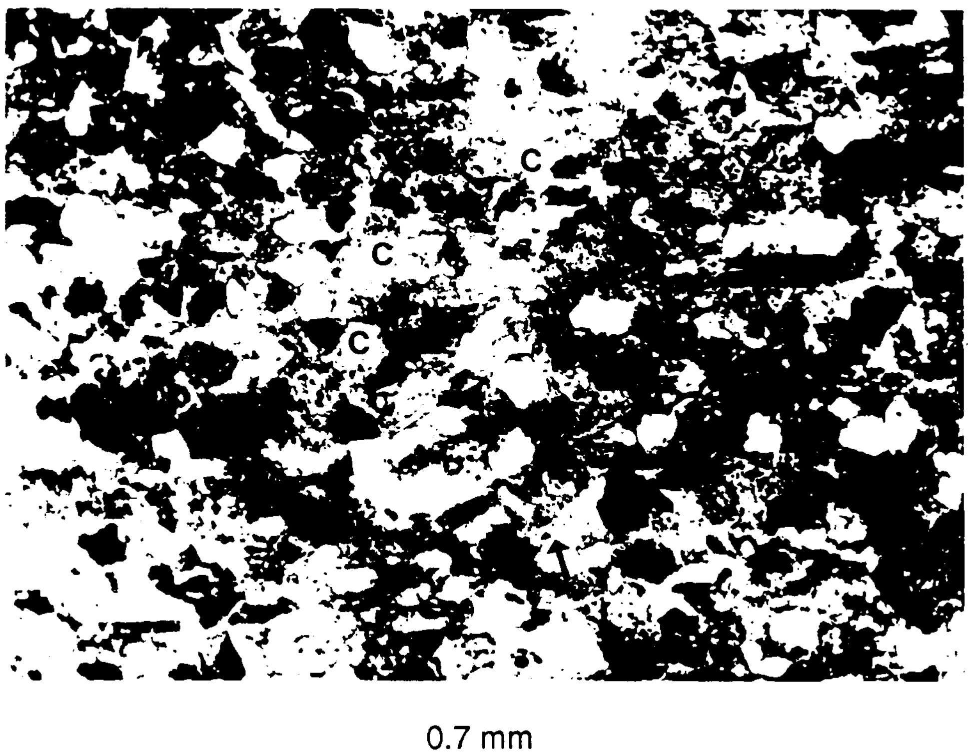

Figure 9: Calcite-cemented fine-grained sandstone layers from the silty-clay shale lithofacies. Intergranular calcite cement (C) is poikilotopic and exhibits unit extinction. Note calcite replacement of quartz grain (arrow). Parsons Lake 5.2, cross-polarized light.

mica-rich lamellae. Complete point-count data is given in Appendix B.

Siltstone-shale lithofacies

Core observations

The siltstone-shale lithofacies is composed of lenticular laminations of siltstone and fine-grained sandstone interbedded with shale. Siltstone and sandstone layers have a wide range of morphologies, exhibiting single or connected lenticular and parallel laminations, wavy bedding, climbing ripples and small scale flaser beds (Figure 10). Laminar, trough or festoon cross laminations are often present within sandstone and siltstone layers greater than .25 inch (5 mm) thick. In many cases, bioturbation may have significantly reworked laminations resulting in a mottled appearance. Siltstone beds are quartz rich and are commonly carbonate cemented. Intervals of herringbone cross-bed sets greater than 1.25 inches (3.0 cm) thick are present, as are layers of convoluted and overturned bedding.

Plant fragments up to 2.5 inches (6.0 cm) are quite common in the siltstone-shale lithofacies and are commonly surrounded by brown oxidization halos. Fossil material is sparse although small bivalves and brachiopods can be found concentrated in certain layers. Brown siderite nodules are present in some samples. This lithofacies was observed in the Heilman, Kinne, Gaddy, Olson and Hardin cores.

Outcrop observations

The siltstone-shale lithofacies was observed in outcrop only at the Lower Coffeyville Section where 1.5 feet (0.5 m) is present. Thin siltstone flaser beds

Figure 10: Common sedimentary structures of the siltstone-shale lithofacies. laminations of siltstone, wavy bedding and thin (<5 mm) flaser beds. Small-scale cross lamellae can be present within the siltstone layers (arrows) and may have multidirectional cross-lamellae. Middle Ladore. Gaddy, 314' 6".

and climbing ripples are interbedded with shale and exhibit cross laminations similar to those seen in core. In outcrop this lithofacies grades upwards into fine-grained sandstone.

Microscopic analysis

Analysis of the thin-sections reveals the presence of two distinct fabrics within this lithofacies. The dominant fabric shows lamellae of shale mixed with thin beds of coarse-grained siltstone or fine-grained sandstone, which are generally less than .25 inch (1.0 cm) thick. Sand grains in the sandstone or siltstone layers are rounded to sub-angular. They are either tightly packed or cemented with large poikilotopic crystals of ferroan calcite which occlude porosity.

Muscovite grains are present in sandstone and siltstone layers and show evidence of being crushed or altered to clays (Figure 11). Pore-filling clays make up less than 10% of these siltstone and sandstones and have been identified as a mixture of kaolinite and illite based on crystal morphology and EDX data. Plagioclase is the dominant feldspar and composes less than 10% of the silt / sand layers. Feldspars are altered to kaolinite and occasionally illite (Figure 12). Ostracodes, forams and crinoid fragments are rare, and when present, are neomorphosed or micritized. Organic stringers and pyrite occur as thin laminations.

Shale layers are intermixed with the fine-grained sandstones and siltstones described above, and are dominantly composed of mica grains, clays, organic material and pyrite. Muscovite and biotite present in thin laminae exhibit unit extinction along the length of the shale layer (Figure 13). The alternation of these mica-rich shale layers with the coarser-grained layers result in cross-stratification

0.4 mm

Figure 11: Muscovite grains in siltstone (of siltstone-shale lithofacies) bent around quartz grains. Note the conversion of micas (M) to illite (I). Lower Coffeyville 14.5. cross-polarized light.

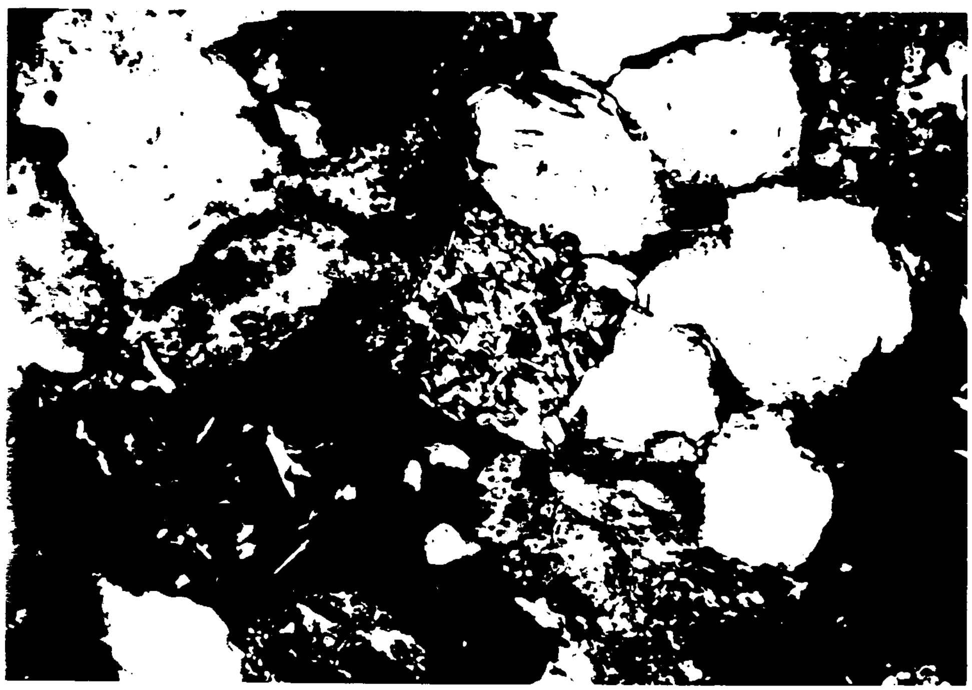

0.1 mm

Figure 12: Feldspar grain completely altered to kaolinite. Clays maintain the original shape of the detrital grain. Hardin 171' 0"s, cross-polarized light.

0.4 mm

Figure 13: Shale lamellae composed predominantly of parallel muscovite grains within siltstone-shale lithofacies . Note unit extinction of shale lamellae (S), and poikilotopic calcite cement (C) present in siltstone layers. Hardin 171' 0"s, cross-polarized light.

visible at macroscopic scale. Shale mixed with coarse-grained siltstone and fine-grained sandstones are present in the Gaddy, Hardin and Kinne cores and the Lower Coffeyville outcrop. The second fabric present in the siltstone-shale lithofacies consists of fine-grained sandstone layers without shale laminations. The most distinct difference in this fabric is the lack of intergranular poikilotopic calcite cement in the sandstone layers. Grains are rounded to sub-angular, and quartz grains often show quartz overgrowths (Figure 14). Orthoclase is the dominant feldspar composing up to 10% of the rock volume, while total feldspar content ranges up to 22 percent. All feldspars show some degree of pitting or partial dissolution and are commonly associated with illite or sericite. Patchy ferroan calcite cement is present in some samples, and where absent, primary and oversized secondary pores are found, generally making up less than 5 percent of rock volume. Organic material including wood fragments, occur in layers, causing a streaked look in thin-section (Figure 15).

Sandstone lithofacies

Core observations

This lithofacies is represented by beds less than 5 feet (1.5 m) thick of fine to very fine-grained sandstone with massive, wavy or laminated beds or herringbone cross-bedding (Figure 16). Thin, gray-shale drapes (<.5 inch, 1 cm thick) within the sandstone are common. Black, carbonized plant fragments and mica grains commonly occur on bedding surfaces. Bioturbation and some soft-sediment deformation such as overturned or recumbent bedding is present in this lithofacies. Rounded siderite pebbles and brown siderite nodules are rarely present. These sandstones are often abruptly overlain and underlain by units of

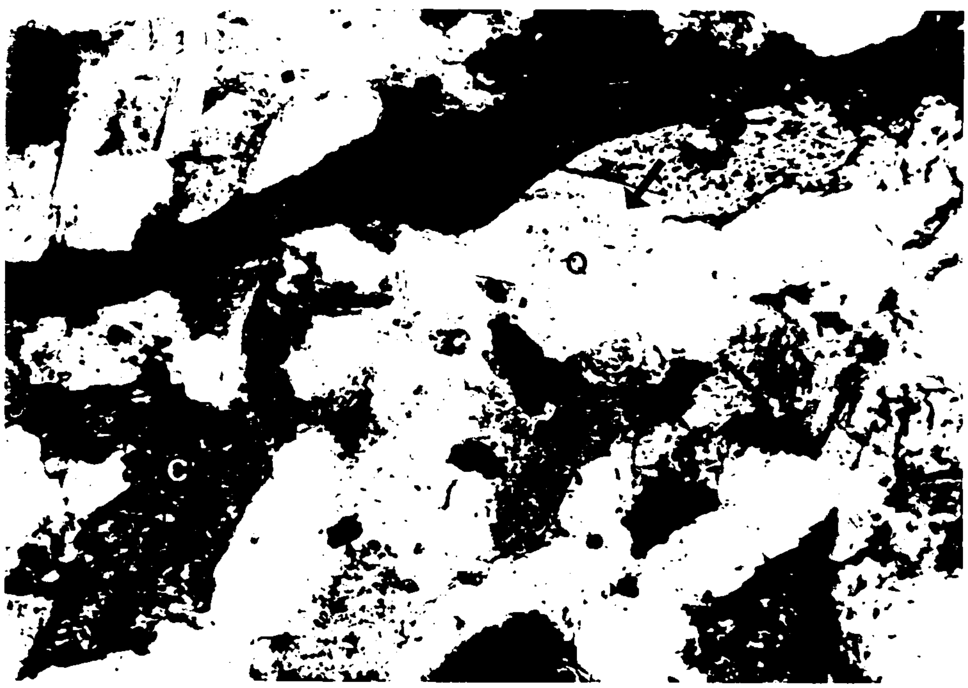

0.4 mm

Figure 14: Euhedral quartz overgrowth on detrital quartz grain. Dust rim (arrow) delineates the boundary between host grain and overgrowth (Q). Pore space is colored light blue. Note pore filling calcite (C) in lower right hand corner. Sandstone fabric of the siltstone-shale lithofacies. Hardin 155' 6"s, plain light.

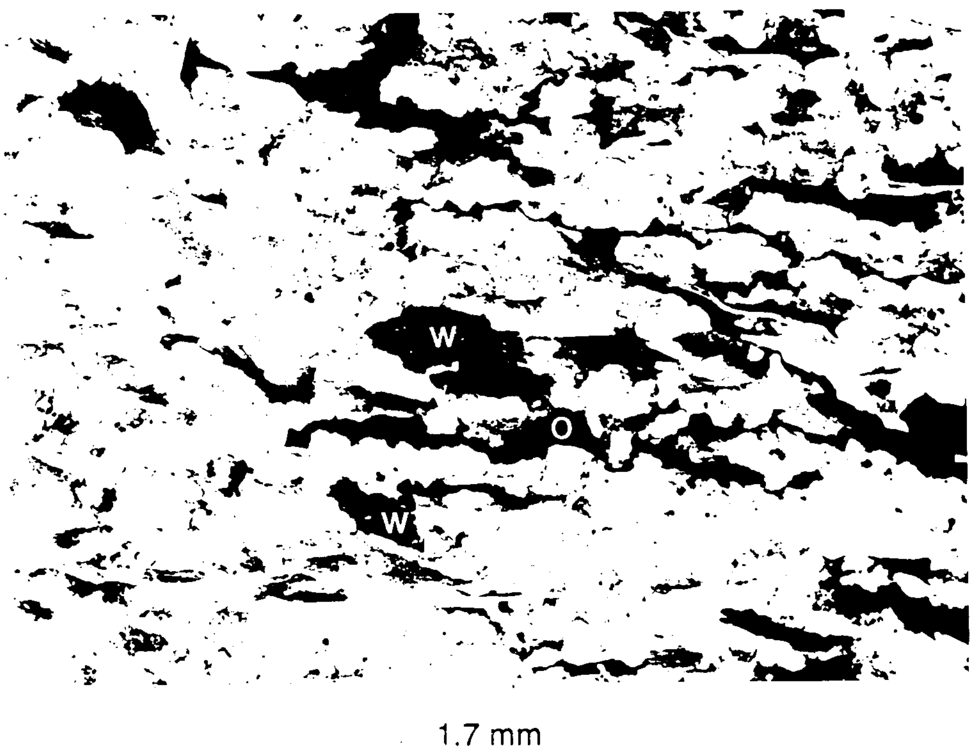

Figure 15: Plant fragments and organics (O) present in the siltstone-shale lithofacies. Note cellular structure of woody plant fragments (W). Sandstone fabric of the siltstone-shale lithofacies. Hardin 155' 6"s, plane light.

Figure 16: Thick sandstone bed of the sandstone lithofacies. Note common flaser beds on left and the abrupt contact (arrow) with the overlying siltstone-shale lithofacies. Large brown object (S) is siderite nodule. Top of core is upper left, bottom is lower right. Hardin core, 156' to 166'.

the siltstone-shale lithofacies. The O.G.S. Hardin core is the only subsurface sample location where this lithofacies is present (Figure17).

Outcrop observations

The sandstone lithofacies crops out as a 4 foot (1.2 m) thick ripple-laminated fine grained sandstone at the Lower Coffeyville section near Sapulpa, Oklahoma. Cross bed sets have a height of approximately 2 inches (0.05 m) and a width of 3 to 4 inches (0.08 to 0.1 m). The sands are poorly cemented and are stained reddish brown. Plant fossils and nodules were not observed.

Microscopic analysis

Units that compose the sandstone lithofacies are made up of well-rounded to angular, fine and medium-grained sandstones. Samples from outcrop show mineralogical differences compared to core samples, notably the lack of poikilotopic ferroan calcite cement in outcrop compared to common occurrence in core samples. Ferroan calcite cement in outcrop samples is negligible, but can form up 20 % of subsurface samples of this lithofacies. Another distinction between core and outcrop specimens is that outcrop samples contain ubiquitous pore-filling iron oxide and iron-stained patches, which give them an overall brownish-red color while core samples contain only trace amounts of iron oxide.

Authigenic clays such as kaolinite, illite and chlorite are common and can take a variety of forms, such as: grains with discrete boundaries, crushed grains, incompletely altered grains, grain coatings, or pore fillings that may contain significant intragranular porosity (Figures 18, 19, 20). Taken together, clays compose about 7% of outcrop samples and between 2 and 10 % of sandstones from core.

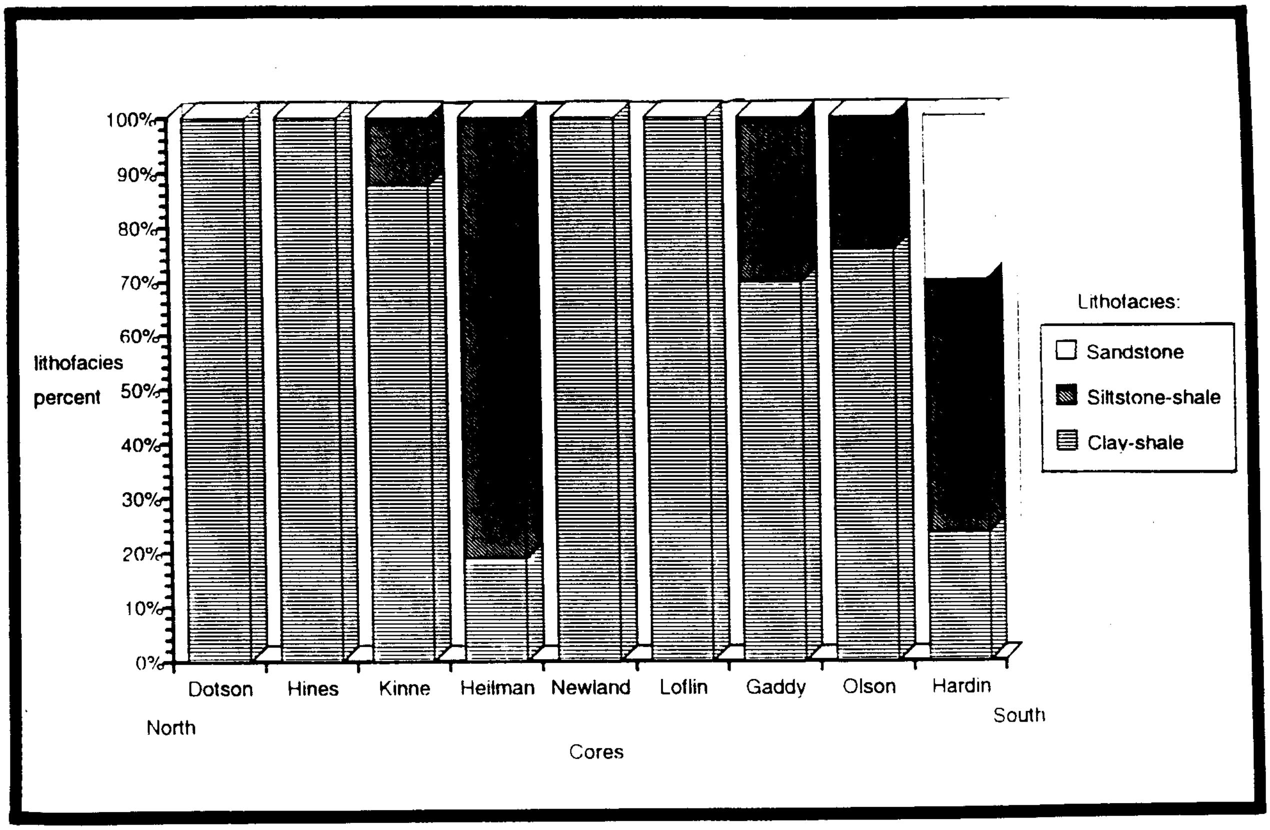

Figure 17: Histogram showing relative percentages of lithofacies in each core. Cores are arranged from north (left) to south (right). Note general increase in siltstone-shale lithofacies in three southern most cores,and that the sandstone lithofacies is present only in the most southern Hardin core.

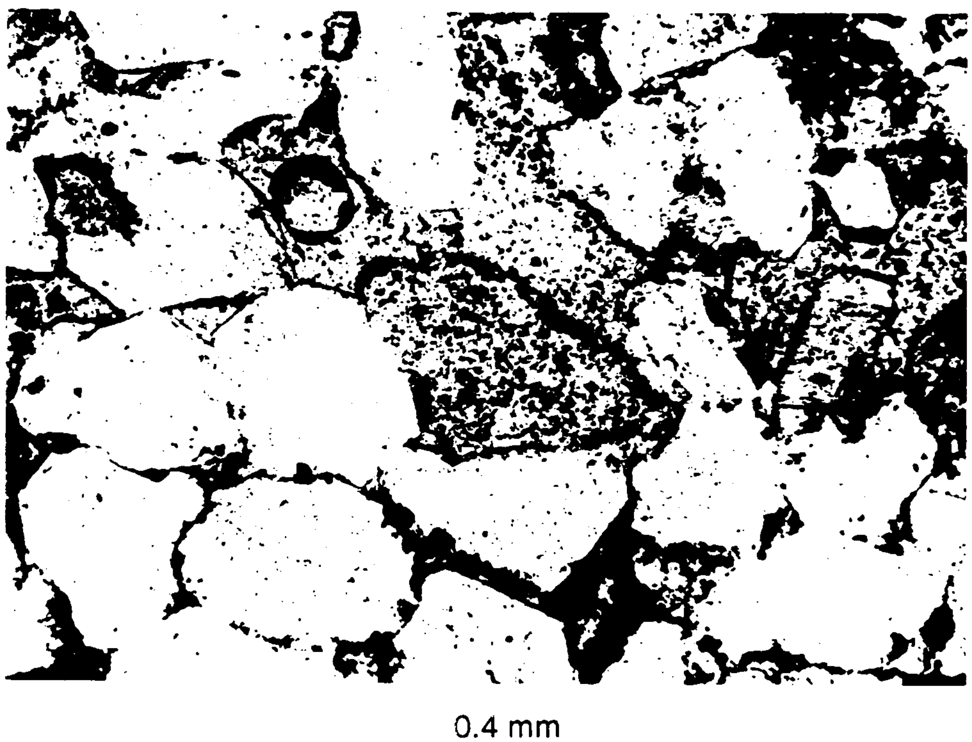

Figure 18: Detrital grain, possibly orthoclase, converted to kaolinite (K). Lower Coffeyville 16.0, plane light.

Figure 19: Same as figure 18 with crossed polarizers. Note complete alteration to kaolinite. Lower Coffeyville 16.0, cross-polarized light.

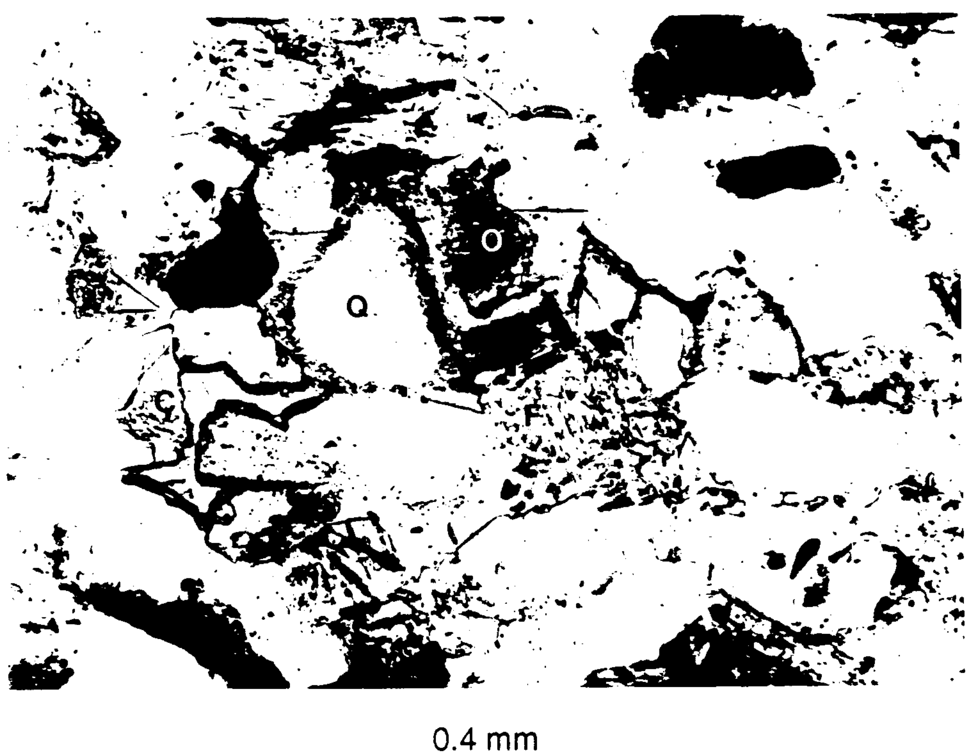

Figure 20: Several types of clay morphologies present in the sandstone lithofacies. Clay coating of illite (arrow) surrounding quartz grain (Q). Plagioclase feldspar grain (F) showing partial dissolution, and weathered orthoclase grain (O) partially converted to kaolinite. Patch of pore filling calcite cement (C) is partially replacing quartz grain. Note, light blue color is pore space filled with polyester resin. Hardin 165' 9", plane light.

Feldspars compose less than 6% of outcrop samples and average roughly 10 % of cored sandstones. Orthoclase feldspar grains are the most common, and almost always are pitted or partially dissolved, while plagioclase grains commonly show evidence of dissolution (Figure 20). Organic matter is often associated with pyrite, and both minerals are present in thin stringers, often in mica-rich layers. Iron rich "box-work structures" have subparallel fibrous strands and can fill up to 7% of pore spaces and are present only in the Lower Coffeyville section (Figure 21).

Quartz overgrowths are present in outcrop, and can be quite large and well developed in cores, notably in sandstones from the southern Hardin core and Lower Coffeyville section in Oklahoma. Primary porosity in these sandstones can range from less than 1% up to 15%, while secondary porosity varies widely among samples (from 1% to 9%) and may have been effected by leaching of calcite cement and formation of quartz overgrowths as discussed in the diagenesis chapter.

Unaltered metamorphic rock fragments, chert and sedimentary pebbles are found in low abundance in these sandstones, except for one sample , where shale chips compose 22 % of the thin-section.

Figure 21: 'Box-work' iron oxide structures found in outcrop samples of the sandstone lithofacies. Fibers of hematite span the width of this pore and intersect at roughly 60° and 120°. Lower Coffeyville 16.0, plane light.

DEPOSITIONAL ENVIRONMENTS

The depositional environments of the Ladore Shale were interpreted by considering three diagnostic characteristics of these rocks: 1) the regional thickness variations of the Ladore, as seen in an isopach-thickness map, 2) distribution of lithologies in cross-section; and 3) sedimentary structures and dominant grain size of the units within each lithofaces.

Diagnostic characteristics

Thickness variations

An isopach map (Plate 1) was constructed for the Ladore Shale based on thicknesses obtained from well-logs and cores. This map encompasses the northern most extent of the Ladore, to the southern most limit where the Ladore Shale can be distinguished as a discrete unit within the Coffeyville Formation. Southward of this line, the Galesburg Shale and the Ladore Shale are not separated by the Mound Valley Limestone, but the thickness of both these units together increase southward.

This map provides: 1) a framework for interpreting lithologic changes and distribution of depositional lithofacies in the Ladore Shale, 2) the overall configuration of the depositional site for the Ladore Shale, and 3) potential paleosource for these sediments.

The Ladore Shale is interpreted to have been deposited within a deltaic system that prograded across the margin of a shallow inland sea. The overall geometry of this unit shows thickening towards the east-southeast, which is interpreted to be the siliciclastic source direction. The thickening of a unit towards the depositional source is the dominant characteristic of a deltaic deposit in an interior basin, and all sedimentary facies present in deltaic deposits are characterized by this geometry (Visher et. al., 1980).

The boundary marking the northern edge of the Ladore may represent the farthest extent of the transportation and deposition of fine-grained material in this inland sea. The isopach map shows a number of lobe-shaped areas where the Ladore thickens in a few miles (<5 km) from less than 20 feet (6.1 m) to greater than 80 feet (24.4 m) in thickness. These features probably represent deltaic lobes that prograded across the shelf during low stands of sea level. The thickest deposits are in the east-southeast portion of the study area and appear to represent distributary channel or lower fluvial-valley deposits, and most likely represents the source of sediments that make up the Ladore Shale. This thick portion of the Ladore is exposed at the surface along the outcrop belt in southeast Kansas and northeast Oklahoma.

The sediments that compose the Ladore Shale can be characterized as having a lobate geometry, which indicates a deltaic system that may have been highly constructive (Fisher et. al., 1969). This system was dominated by fluvial input of sediments, while wave and longshore drift processes were probably not reworking the majority of the sediments being deposited. The isopach map of the Ladore Shale shows a lack of coastal barriers which are generally found in high-destructive deltaic environments.

Distribution of lithofacies

Each of the three lithofacies has a unique distribution and subsurface extent, which appears to be a function of the distance from the paleo-source for these sediments. Based on sedimentary structures and grain-size, the finer-grained lithologies seem to represent sediments deposited in the distal portion of the deltaic system, while coarser-grained lithologies represent deposition in the proximal part of the system.

Figure 22 illustrates a cross-section of the Coffeyville Formation across southeastern Kansas, which was constructed based on cores and well log data. The three Ladore lithofacies exhibit a general increase in grain-size towards the south, but are not found in a discrete order and often exhibit alternation between the fine silty-clay shale lithofacies and coarser grained silty-shale lithofacies over short distances within core and outcrop samples. This alternation of lithofacies may represent the fluctuating dominance between fluvial processes, which may have deposited the siltstone and sandstone-rich lithofacies, and marine process such as sedimentation from suspension, which probably deposited the shale-rich portions of these lithofacies. In addition, sediments may have been substantially reworked as deltaic lobes prograded over the previously deposited prodeltaic or distributary-mouth bar sediments. This reworking of sediments after initial deposition may have removed some or all of a particular lithofacies and may help to explain the sudden lateral changes in lithofacies present in the Ladore Shale when seen in cross-section.

The silty-clay shale lithofacies is the most abundant lithology, making up the largest percent of most cores sampled for this study (Figure 17). In addition, this lithofacies has the widest distribution in outcrop and in the subsurface, being

Figure 22: Cross-section A - A' across southeast Kansas and northern Oklahoma (northeast to southwest). Note increase in silt and sand-dominated facies towards the south and lateral variations in lithology, most likely due to fluctuating dominance between fluvial and more open marine processes.

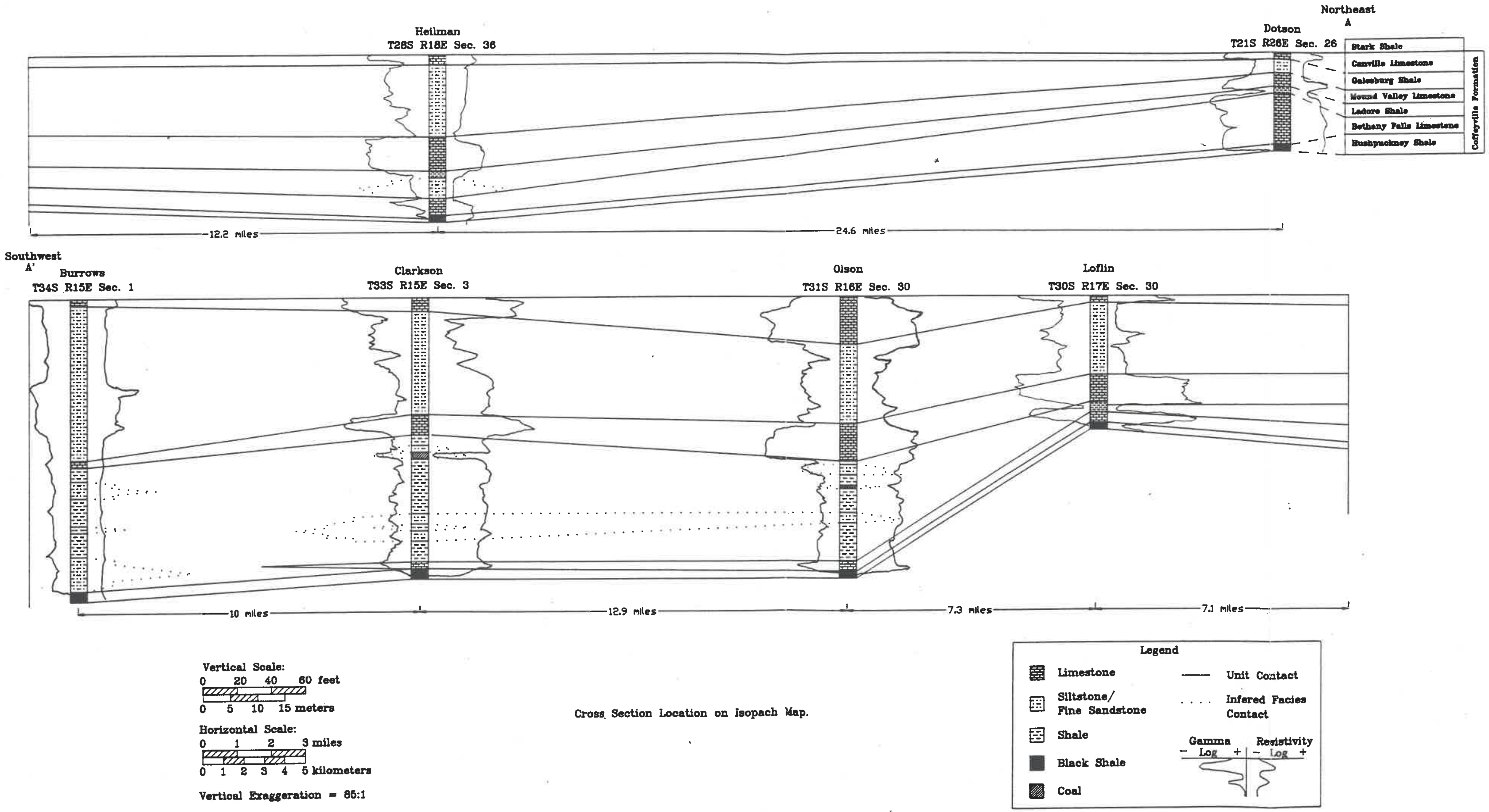

Cross Section Location on Isopach Map.

present from the northern to southernmost cores and outcrops. Along the northernmost edge of the Ladore these shaley units are thin and calcareous, while to the south-southeast the siltstone and sandstone content increases.

The siltstone-shale lithofacies shows a general increase in frequency and thickness towards the south (see Figure 17), while the sandstone lithofacies is present in only limited areas in two southern locations, and is absent north of the Kansas-Oklahoma boarder. In cross-section, these lithofacies are seen as lens-shaped silt and sand-rich units with limited lateral extent.

Sedimentary processes

Silty-clay shale lithofacies

The dominant sedimentary structure of this lithofacies are fine laminations (<1 mm) of the silty-clay shale, and the almost complete lack of siliciclastic material coarser than fine-grained silt. In these shales, plant fragments, bioturbation, color-banding and siderite nodules are common. Thin layers of micrite, skeletal debris and calcite-cemented siltstone are rare but where present, are in laterally continuous thin beds. Occasional beds of starved ripples of fine-grained siltstone are present in this lithofacies as well.

The thin laminations of silty-clay shale represents slow deposition from fine-grained suspended material in an environment not greatly effected by wave or current energy, most likely a prodeltaic environment grading upwards into a delta-front environment (Figure 23). The limited presence of burrows indicates a rapid accumulation rate of sediments that allowed allow sediment feeders to live in the substrate, but deposited enough sediment to prevent thorough reworking by organisms and homogenization of shale lamellae. The abundance of small plant

Figure 23: Dominant depositional environments of the delta which deposited the Ladore Shale. Facies moved north during increased fluvial discharge and receded south when fluvial discharge decreased, accounting for wide-spread distribution of Ladore lithofacies. Silty-clay shale lithofacies deposited in prodeltaic facies and delta front facies, siltstone-shale lithofacies deposited within distributary mouth bar and distal bar facies, sandstone lithofacies deposited in distributary channel facies.

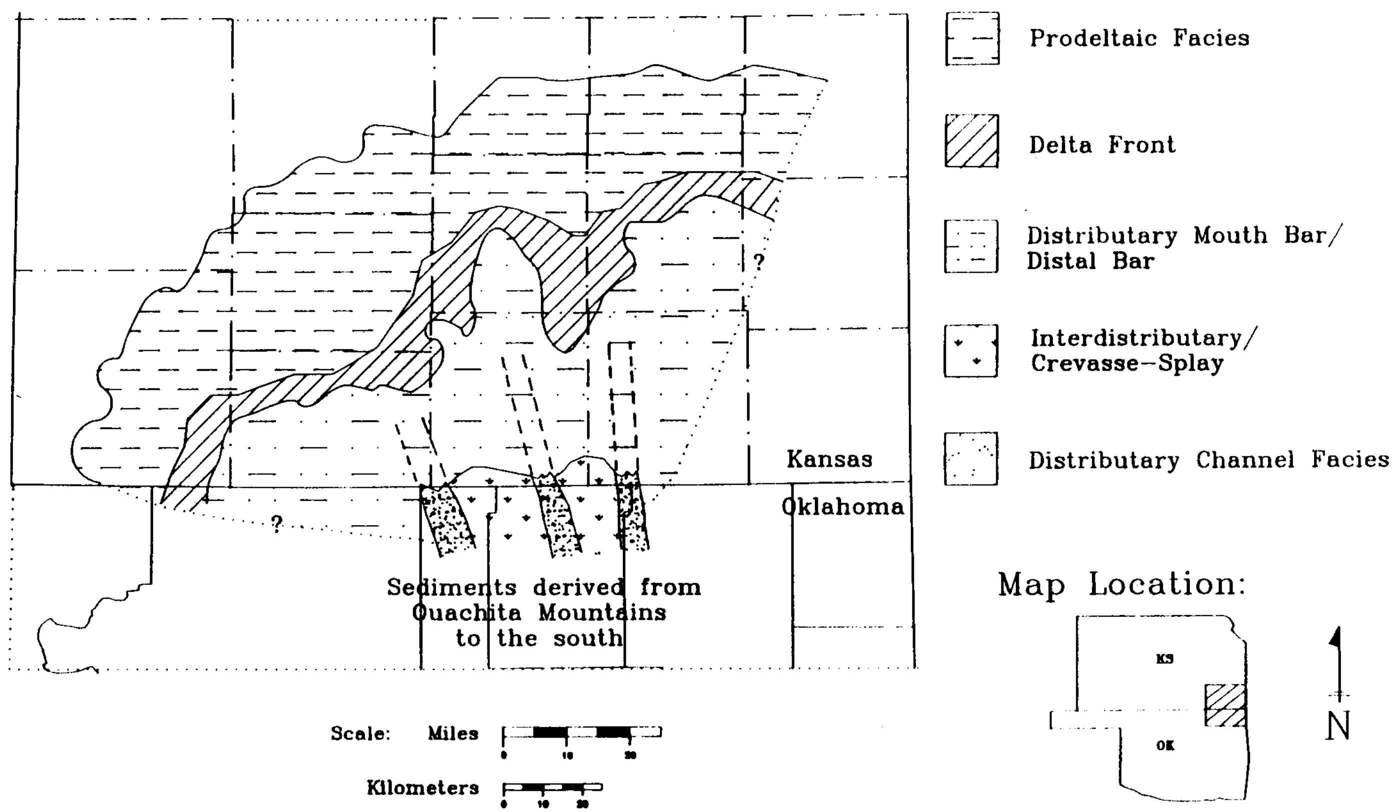
Prodeltaic Facies
Delta Front
Distributary Mouth Bar/
Distal Bar
Interdistributary/
Crevasse-Splay
Distributary Channel Facies
Kansas
Oklahoma
?
?
Sediments derived from
Quachita Mountains
to the south
Scale: Miles
Kilometers
Map Location:
KS
OK
N

fragments implies a distal relationship to the depositional source as only fine suspended organic material would be transported large distances away from the river mouth. The great abundance of plant fragments in this lithofacies of the Ladore Shale implies rapid accumulation rate and low oxygen content of water in the basin. The partial decay of organics may have decreased the oxygen in these waters, which prevented the complete oxidization and breakdown of plant remains. Color variations present in this lithofacies between brown shale and gray-black shale as seen in figure 4, may indicate changes in water chemistry in the outer transitional-marine environment (Coleman and Gagliano, 1965).

Rare but continuous layers of micrite or skeletal debris represent changes in the depositional environment beyond the delta-front. A major lithologic change is represented in the sudden transition from detrital sedimentation to carbonate deposition, as indicated by the abrupt boundaries between carbonate beds and the units surrounding them. These carbonate layers were deposited when clastic influx was temporarily cut off, possibly due to delta-lobe switching or due to a decrease in river discharge, which lowered sedimentation rate at the distal and medial portions of the delta front. This decrease in clastic sedimentation rate allowed carbonate precipitation and accumulation as laterally continuous beds that may have covered a large portion of the delta area.

Lithologic changes may have been accompanied by salinity changes. The fauna present in these carbonate beds is composed of both potentially euryhaline organisms, such as ostracodes, gastropods as well organisms less tolerant of salinity fluctuations, such as brachiopods and crinoids (Heckel, 1972). This suggests that salinity may have decreased as fresh water dominated due to influx from nearby lobes, then changed back towards normal marine from the diversion of fluvial waters and sediments which allowed the substrate to be recolonized by fauna that could not survive on an detlaic lobe dominated by fresh waters.

Fine-grained siltstones or very fine-grained sandstone with climbing ripples are rarely present in this lithofacies, and most likely represent increases in sedimentation rate and current velocity. Cross-stratified structures present in these siltstone and fine-grained sandstone beds may have been formed in response to increased sedimentary influx. This clastic influx of relatively coarse-grained material represents the penetration of the delta-front environment and may have resulted from increased river discharge or temporary lowering of wave-base, thereby allowing wave energy to rework the substrate, winnowing out fine-grained sediment. Ostracodes are the only shell fragments present in these silty lamellae, and the lack of other organisms may indicate deposition of sediment derived from an environment dominated by freshwater, and fluvially derived clastic material.

At the Parsons Lake section, at least one thin coal (6 inch, 15 cm thick) and underclay was observed, while within the Olson core a thin coal (1.5 foot, 0.46 m) is present which is underlain by an interval of brown-mottled mudstone. Both of these coal units are overlain by laminated beds of the silty-clay shale lithofacies. These sub-coal horizons and the associated mottled mudstone units most likely represent a marshy bay-fill or crevasse-splay deposit, which aggraded above sea-level allowing the formation of these thin coal beds. After detrital material was cutoff, possibly due to the abandonment of this crevasse-splay, plant debris accumulated to form the coal, then the area subsided and marine sedimentation processes resulted in the deposition of the overlying delta front and prodeltaic units.

Siderite nodules are common throughout the silty-clay shale lithofacies, are less abundant in the siltstone-shale lithofacies, and are rarely found in the sandstone lithofacies. These carbonate concretions probably formed in a number of different depositional environments soon after deposition of these units, as indicated by their distribution in all three lithofacies. Formation was most likely due to the presence of organic matter, and is discussed in the diagenesis chapter.

At several outcrops orange-gray mottling was observed at the top of the Ladore Shale, near the contact with the Mound Valley limestone. These color and texture variations are observed only in outcrop, but not in core, hence do not represent a change in the depositional history of the Ladore. They are the result of recent weathering of the shale caused by groundwater movement along the Mound Valley-Ladore Shale interface.

Siltstone-shale lithofacies

The sedimentary structures of the siltstone-shale lithofacies can be characterized as containing wavy and lenticular-laminated siltstones and fine-grained sandstone intercalated with silty shale. Bioturbation of sediment layers is common, and can be intense enough to disrupt bedding and homogenize sediments. Plant fragments are ubiquitous, and can be greater than 2.5 inches (0.06 m) in size, while calcareous fossil remains, except for bivalves, are rare.

The interbeds and interlamination of siltstone and sandstone with shale reflects the changing wave and current energy conditions present during deposition, which most likely took place along a seaward-sloping delta front, within a distal bar and distributary mouth bar facies. This facies is associated with shoaling conditions just seaward of the river discharge, where decreasing river velocity reduced river competence, resulting in rapid deposition. These cross-bedded sediments deposited near the seaward edge of the distributary channel would most likely be subject to periods or reworking by stream currents during periods of high river discharge, and by waves generated in the more open-marine setting seaward of the delta front. The rapid sediment influx may have overloaded water-laden sediment, causing slope failures as sediments moved seaward, which produced the overturned, recumbent bedding, which is present in some places in this lithofacies, similar to the features described by Coleman and Prior (1982) in modern deltas. The multidirectional stratification within siltstone and sandstone lamellae, herringbone cross strata, and the prevalence of flaser beds might be do to reworking of these deltaic sediments during a period of tidal flat deposition. Shoaling conditions seaward of the river discharge allowed these fluvially deposited sediments to be reworked and redeposited by tidal activity.

The laminated silts of this lithofacies probably reflect an increase in river-current discharge, possibly due to periodic floods, while shales were deposited during lower discharge periods.

Coleman and Gagliano (1965) note that in the modern Mississippi river delta bars, the dilution of salinities by nutrient-rich river water creates favorable conditions for burrowing organisms tolerant of salinity fluctuations, particularly bivalve mollusks. This may explain the intense burrowing and presence of bivalve fragments as the most common type of fossil. Also, in these units plant fragments can be quite large, indicating a more proximal location to the source of sediments, compared to the silty-clay shale lithofacies.

Sandstone lithofacies

The sandstone lithofacies is composed of fine-grained sandstone beds which exhibit a variety of sedimentary structures, such as wavy laminations, herringbone cross-bedding and homogeneous beds. Flaser beds (<5 mm thick) and beds of siltstone (<10 cm thick) can be intermixed with sandstone layers. Plant fragments are common on bedding planes. Some layers of sandstone and shale show recumbent lamellae and other evidence of disturbed stratification.

This lithofacies is interpreted to have been deposited as a distributary channel sand, in the lower delta plain landward of the distributary mouth. The relatively coarse-grained lithology of this sandstone and massive beds indicates bed-load transport of sediment by flowing water in the distributary channel.

Siderite pebbles in at least one instance, are concentrated in layers near the base of a sandstone bed. These rounded pebbles are mixed with abundant large plant debris, and the bed is bounded by an erosional base. This sandstone bed most likely represents a channel lag deposit, which remained after currents scoured out the underlying silts and shales below during channel emplacement, similar to channel lags observed by Swanson (1979) in other Pennsylvanian sandstones. The siderite pebbles are most likely recycled siderite nodules that were previously deposited in shales, and which were eroded out and rounded during transport in the distributary channel. Large pieces of plant material were also deposited in this channel lag and may represent water-logged plant debris that was concentrated in this channel-lag deposit.

The disturbed strata present may have been the result of gravity induced slumps that formed along channel walls or from silt-laden currents that flowed along the channel bottom, possibly during low water periods similar to those described in the modern by Coleman and Gagliano, 1965. The thin clay-shale partings that commonly separate sandstone beds may also have been deposited by sluggish currents during low river stages as fine material dropped out of suspended load and was deposited over sandy channel deposits.

DIAGENESIS

Diagenetic effects

The sandstones and siltstones of the Ladore shale have undergone diagenetic modifications that include: the formation of authigenic cements, alteration of feldspars, partial dissolution of grains and cements, and replacement of detrital grains.

Calcite cement

Calcite cement is the most common intergranular cement in the siltstones and sandstones of the Ladore shale. Two fabrics are present: 1) poikilotopic cement, in the form of large crystals of cement in optical continuity that enclose several grains (Figure 9); and 2) isolated euhedral to subhedral pore-fillings (Figure 14). In the Ladore shale, calcite cement ranges in composition from iron-free calcite to ferroan calcite, which generally contains 2.5 to 3.5 % iron oxide . Ferroan calcite is the most abundant phase of cement, and dolomite was not detected in samples that were studied. Table 2 summarizes the petrographic characteristics of each lithofacies.

The siltstones and fine-grained sandstones commonly contain continuous poikilotopic ferroan calcite cement, which contain 'floating' quartz grains, while coarser-grained sandstones show isolated pore-filling cements or patches of poikilotopic surrounded by secondary pore space.

Within the siltstones and sandstones of the Ladore Shale, replacement of

Table 2: Petrographic characteristics present in the three lithofacies of the Ladore shale. a = absent, r = rare, o = occasional, c = common.

	Diagenetic features								
	Cements:				Grain alteration:				
Lithofacies:	*poikilotopic calcite*	*pore filling calcite*	*quartz overgth.*	*hematite cement*	*feldspar FGA / FGD*	*calcite rep. quartz*	*pyrite*	*authigenic clays*	*dissolved calcite cement*
Silty-clay shale lithofacies	a	a	a	a	a	a	o	c	a
micrite layers	a	c	a	a	a	a	c	a	a
skeletal grain layers	c	a	a	a	a	a	o	a	a
quartz siltsone layers	c	a	a	a	a	a	o	c	a
Siltstone-shale lithofacies	c	o	o	a	o	o	o	o	o
mixed siltstone-shale fabric	c	a	a	a	o	o	o	c	a
fine-grained sandstone fabric	a	c	c	o	c	c	o	c	c
Sandstone lithofacies (core)	o	o	c	a	c	c	o	c	c
Sandstone lithofacies (outcrop)	c	a	c	c	c	c	a	c	c

quartz grains by calcite is suggested by the embayed nature of the edges of some quartz grains. Calcite cement is commonly found as partial replacement of quartz grains, as evidenced by small-scale dissolution features along grain edges (Figure 24) and large scale embayments that truncate fabric in the quartz grain (Figure 25). Petrographic and S.E.M. analysis show dissolution of quartz to be on a small scale, much like the notches described by Burley and Kantorowicz (1986) and the irregular boundaries of Dapples (1971) (Figure 26). Extensive quartz-grain dissolution or ghost-grain boundaries within the calcite cement indicating large-scale removal of quartz were occasionally observed.

Calcite replacement of quartz occurred after deposition of quartz overgrowths as shown by cement stratigraphy The calcite crystals truncate syntaxial quartz overgrowths and the original detrital grain, which also show signs of replacement. This grain-replacement by calcite may have taken place according to the thin-film process outlined by Pettijohn et al. (1987). This process involves the dissolution of quartz by a thin film of water (< 5 microns thick) which is undersaturated with respect to silica (Figure 27). The concentration of hydrated silica is greater within the thin film than outside the film and so a diffusion gradient is formed where hydrous silica is diffused into the pore-waters. At the same time, calcite is oversaturated in pore waters and diffuses into the thin film between the calcite and quartz grains. Calcite is then deposited on the edge of the calcite crystal, thereby replacing the quartz grain. This process could be responsible for the pitting and embayments present on detrital quartz grains and syntaxial overgrowths.

These calcite cements formed as calcium cations and carbonate anions become overstaturated in pore fluids, precipitating calcite in voids. Potential sources for

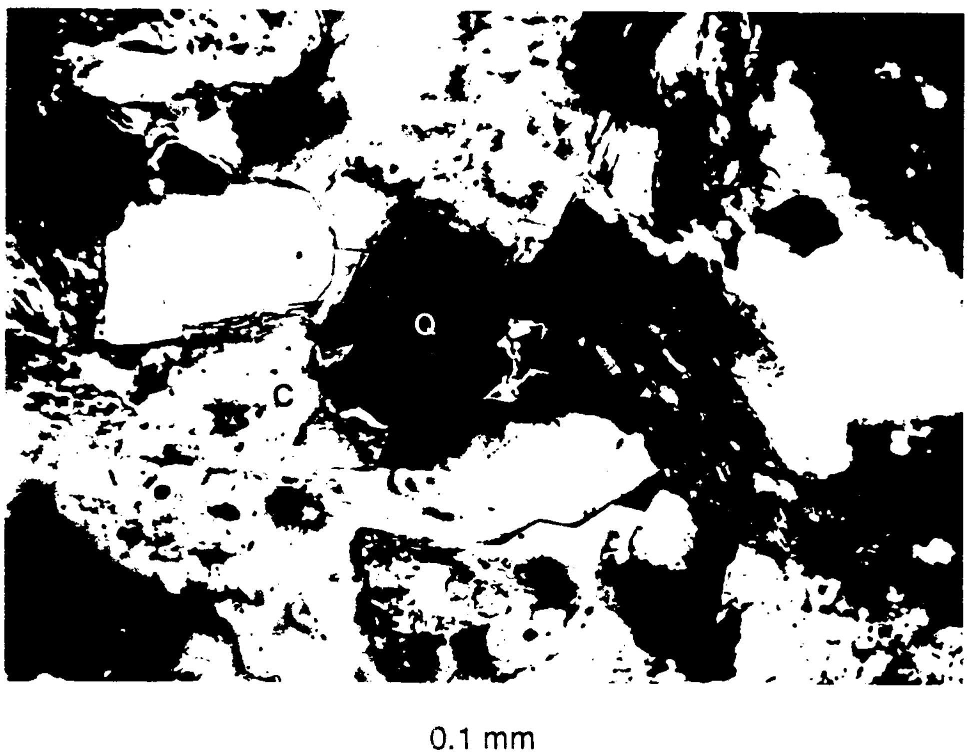

Figure 24: Quartz grain being replaced by calcite along grain boundary. Note that euhedral syntaxial quartz overgrowth covers detrital quartz grain (Q) indicating that quartz cementation occurred before poikilotopic carbonate cement formed. Hardin 169' 8", crossed-polarized light.

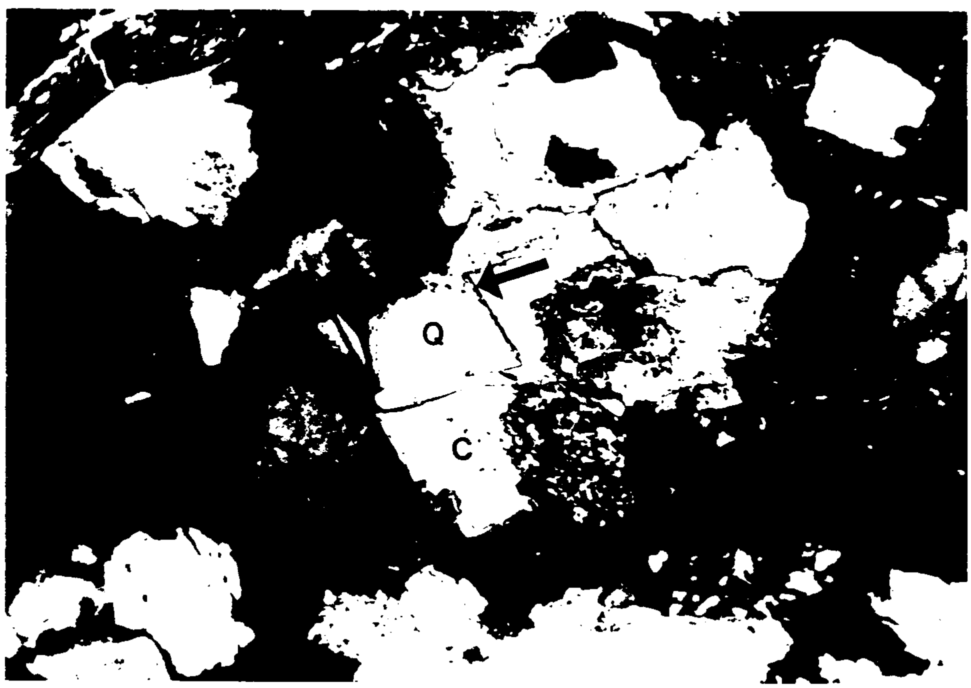

Figure 25: Calcite replacement of quartz. Significant portion of quartz grain (Q) and syntaxial overgrowth (arrow) truncated by calcite cement (C). Hardin 163' 0". crossed-polarized light.

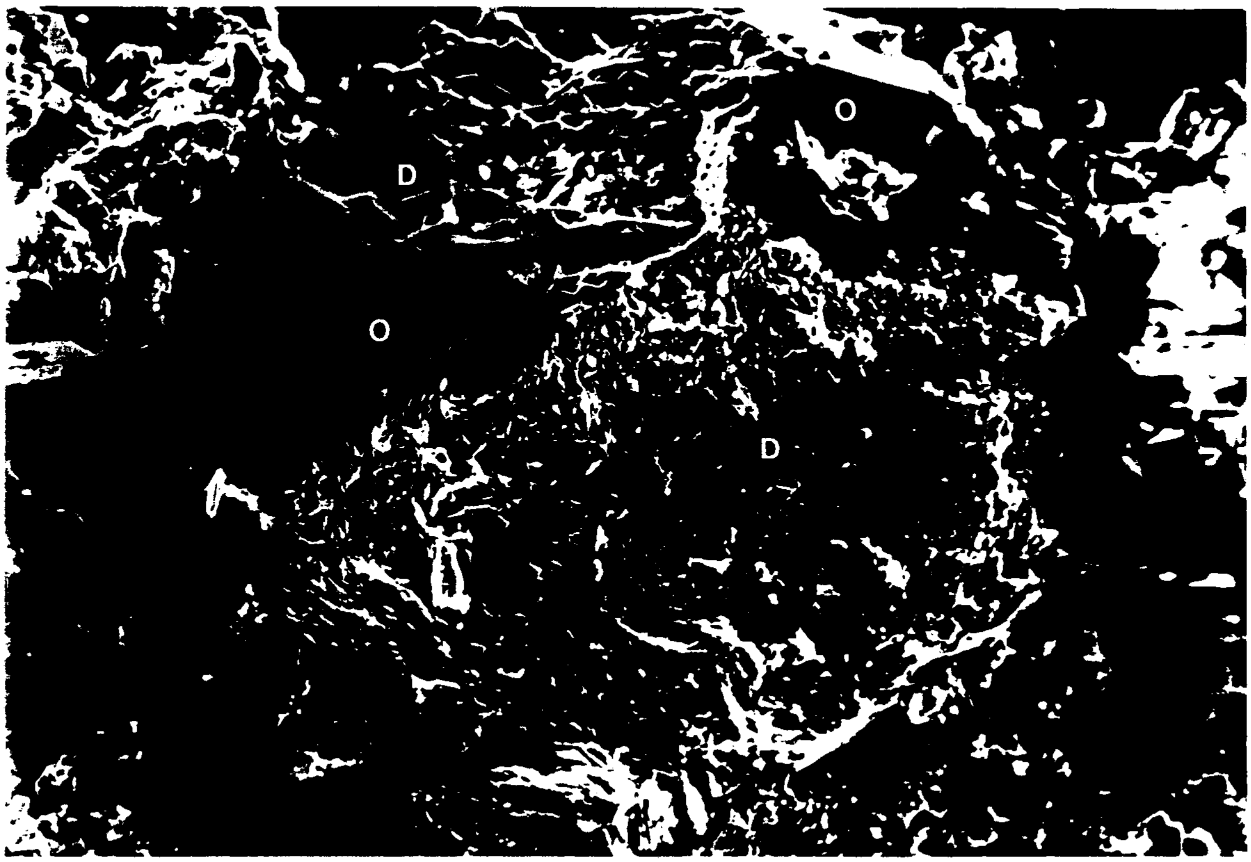

Figure 26: Scanning electron micrograph showing evidence of replacement of quartz by calcite. Quartz overgrowths (O) on detrital quartz grain have been etched by calcite causing large areas of dissolution (D). Calcite has subsequently been dissolved. Ha 159' 6", 5 kv.

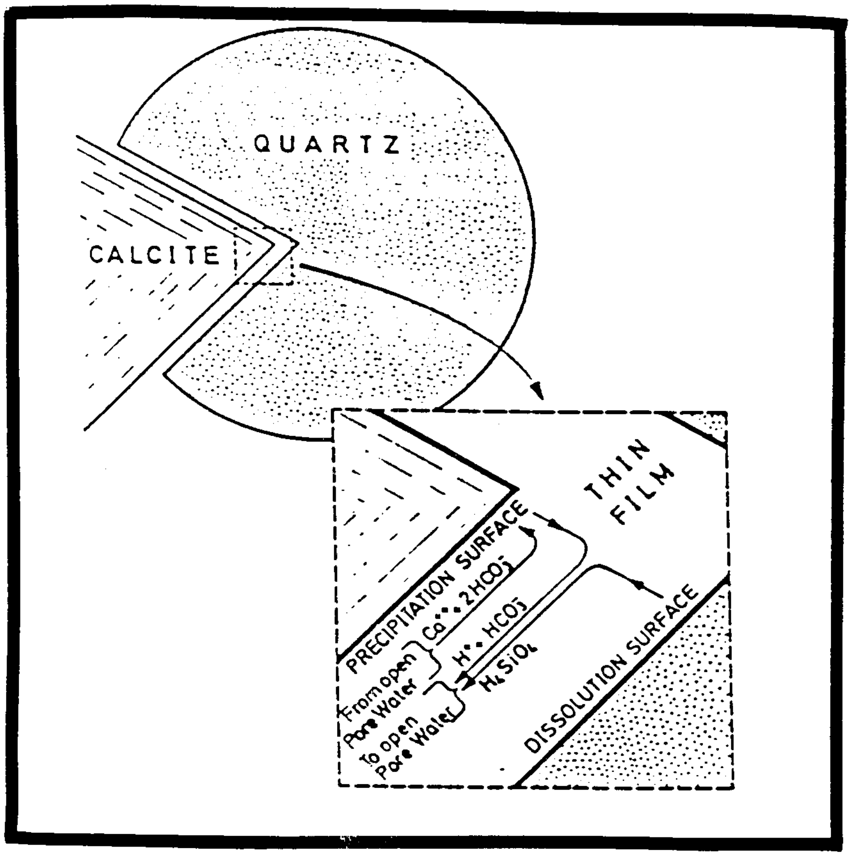

Figure 27: Model for calcite replacement of quartz by chemical transport along a thin film at the replacement front. See text for discussion. From Pettijohn et al., 1987.

these ions include: oversaturated seawater, dissolution of soluble carbonate rocks and clay-mineral reactions (Hutcheon, 1983). The abundance of calcium carbonate in these rocks, as fossils, shell layers and cements and the general lack of carbonate grain dissolution implies supersaturation with respect to carbonate in sea water for some time after deposition. Most likely, these units were initially effected by fresh, potentially acidic waters during deposition, and then after a transgressive event (concurrent with the deposition of the Mound Valley Limestone) these units were bathed in seawater, which was oversaturated with respect to calcite. Poikilotopic cements may have formed by slow precipitation around limited nucleation sites (such as scattered fossil fragments) within the sands, thereby producing the patchy, interlocking framework of calcite crystals. This cementation episode occurred before substantial compaction occurred as evidenced by the illustration of quartz-grains 'floating' in calcite cement due to the low degree of grain-to-grain contacts. In addition, these pore fluids were depleted in oxygen, possibly due to the partial oxidization of the abundant organic material, which allowed dissolved Fe^{+2} to be incorporated into the calcite cements. In medium-grained sandstones, poikilotopic calcite is present only as scattered patches that maintain similar petrographic characteristics to those of the cements in the finer-grained sandstones and siltstones. Secondary porosity is higher in coarser units. In general, the calcite cement of the finer-grained layers is more abundant and is composed of larger crystals, hence fine-grained units show reduced porosity compared to the coarser-grained layer because of the prevalence of cement. This implies that both the finer-grained siltstones and the coarser-grained sandstones were cemented in similar fashions at the same time, but the larger grain size of the sandstones may have facilitated migration of later fluids through these units, dissolving the bulk of the calcite cement and increasing secondary porosity. Fluid flow was restricted in the finer-grained units, thereby decreasing the amount of calcite dissolution and the formation of secondary porosity.

The less common cement fabric, that of pore-filling calcite, is seen in conjunction with sandstones and siltstones that have large numbers of grain-to-grain contacts, and which show other evidence of early compaction such as bent mica grains. Pore-filling calcite cement is the result of a later stage of diagenesis and may be related to the conversion of smectite clays to illite, which releases carbonate into the pore-fluids (Boles and Franks, 1979).

Quartz cement

Authigenic quartz overgrowths are an important cementing agent, particularly in the coarser-grained units of the sandstone lithofacies, although they compose less than 5% of rock volume. These overgrowths are euhedral to subhedral and commonly intergrow to produce a interlocking mosaic of quartz grains (Figure 28). Overgrowths are readily distinguished by their pyramidal terminations and may exhibit a clay dust rim that delineates the border between the detrital grain and the overgrowth (Figure 29). Syntaxial overgrowths can be effected by calcite replacement of quartz as illustrated in Figures 24, 25 and 26.

Potential sources of authigenic quartz include: 1) dissolved silica produced by pressure solution of grains, 2) dissolved silica derived from movement of high pH fluids over quartz-rich sandstones, 3) silica released during the compaction of shales, including the dissolution of clay and silt-sized quartz particles, 4) dissolution of biogenic silica 5) silica released during mineral reactions, such as

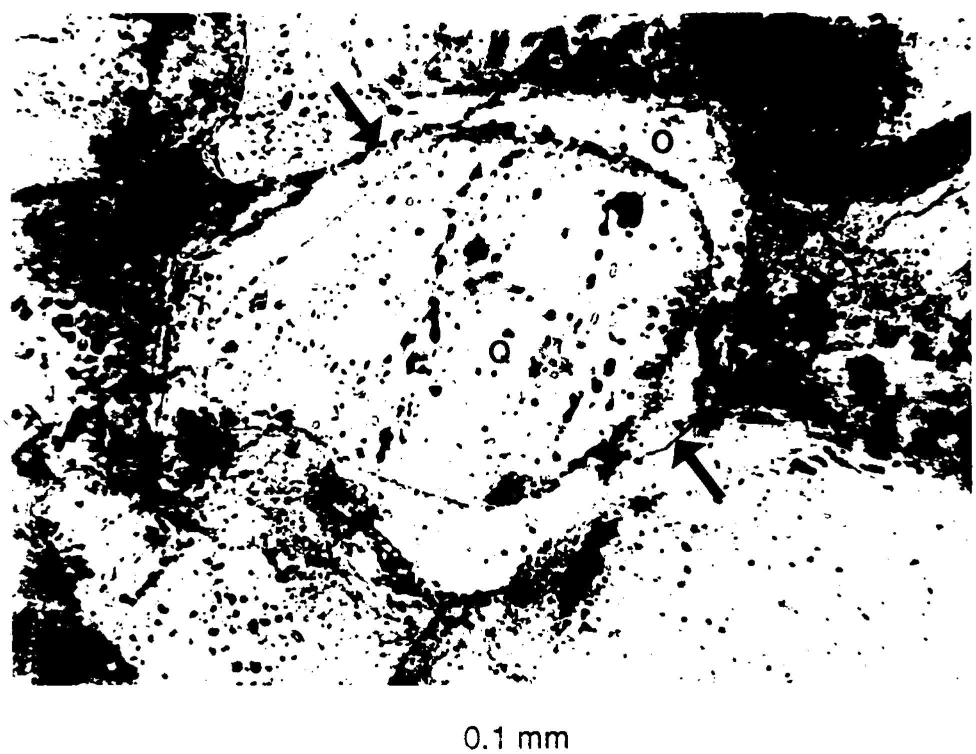

Figure 28: Quartz overgrowth on detrital grain (Q) with pronounced dust rim. Note interlocking nature of this overgrowth (O) with surrounding grains (arrows). Lower Coffeyville 16.0, plane light.

0.37 mm

Figure 29: Scanning electron micrograph of dipyrimidial euhedral quartz overgrowths. Note clays (C) forming 'dust rim' under overgrowth (O). Hardin 159' 6", 5 kv.

the conversion of feldspars to kaolinite, or clay mineral diagenesis (Leder and Park, 1986, Bjørlykke, 1988, Brenner et al., 1991).

Of these possible sources of silica, most can be discounted in these rocks. For example: large scale pressure solution at grain boundaries was not observed in sands from the Ladore Shale. Also, Blatt (1979) showed that precipitation of quartz due to movement of silica-rich water requires unacceptably large volume of pore fluid to pass through rock units, and sources of biogenic silica such as sponge spicules or radiolaria would be unlikely in these non-marine to transitional sediments.

On the other hand, silica released during feldspar diagenesis early in the diagenetic history of these units may have played a major role in authigenic silica formation. The following reaction for the conversion of potassium feldspar to kaolinite illustrates how mobile silica is formed:

$$2KAlSi_3O_8 \text{ (potassium feldspar)} + 2H^+ + H_2O \quad \text{-->}$$

$$Al_2Si_2O_5(OH)_4 \text{ (kaolinite)} + 4SiO_2 \text{ (aq)} + 2K^+$$

In this reaction Na-rich feldspars are altered by H^+, which is present in groundwaters due to vegetative processes (Bjørlykke, 1984). During this conversion, 1 cm^3 of K-feldspar yields 0.46 cm^3 of kaolinite and 0.43 cm^3 of quartz (Leder and Park, 1986). Potassium feldspars such as orthoclase are common in these rocks, whereas microcline is rarely found. Where present, potassium feldspar (microcline) shows significant pitting and dissolution. Kaolinite is commonly found in the sandstones of the Ladore, composing from 1%

to 10% of point-counted samples; this is equal to or greater than authigenic quartz, which makes up a maximum of 2% of these units. Therefore, assuming kaolinite formed according to the above reaction, sufficient dissolved Si^{+4} would be supplied to account for the silica overgrowths of these sandstones . Clay mineral diagenesis is also a possible silica source, as noted by Boles and Franks (1979), and can supply Si^{+4} during the alteration of smectite to illite.

Iron oxide cement

Iron oxide is the least abundant cement in the units of the Ladore shale, and was observed only in outcrop samples. The brownish-red color of hand specimens and thin-sections from the Lower Coffeyville section is caused by iron-oxide cement, which was identified as hematite by crystal morphology and by EDX data. These cements compose 6% on average of the rock specimens from outcrop locations. Samples with abundant hematite cement generally lack poikilotopic calcite cement and have elevated secondary porosity of roughly 6%. Several thin sections have "box-work" pore fillings, fibrous bands of hematite that can span the width of pores. Hematite cements terminate against syntaxial quartz overgrowths indicating that they formed during a later phase of diagenesis.

Core samples show a markedly different distribution of iron oxide compared to outcrop samples. In core samples hematite is present in small amounts, commonly less than 2% of the rock, and does not form cement but rather take the form of grain coatings or pore fillings.

The fact that these rocks do not contain iron-rich minerals in the form of detrital grains, such as pyroxene or amphiboles, suggests another source of iron for cements in these rocks. Also, the common occurrence of hematite in outcrop samples as compared to the uncommon occurrence of iron oxide cements in subsurface rocks suggests these cements are a product of near-surface weathering. Dissolution of ferroan calcite cement , which is common in core samples, in the near-surface environment might have released Fe^{+2} from the calcite, which then oxidized in oxygen-rich meteoric waters forming insoluble Fe^{+3}, which combined with oxygen to produce hematite (Blatt, 1979). The "box-work" nature of hematite cement noted in some samples may represent the concentration of hydrated iron along calcite cleavage planes during dissolution. This could account for the fibrous nature of these pore fillings and the angular nature of some fibers, that intersect at angles of roughly 60 and 120 degrees which corresponds to the cleavage planes of the original calcite cement (Figure 21).

Feldspar alteration

The degradation of feldspars is the most common type of mineral alteration present in the sandstones and siltstones of the Ladore Shale. Feldspars in these units have undergone framework grain alteration (FGA), where the grain is wholly or partially dissolved and the dissolved material is reprecipitated in the surrounding pores as authigenic clays. Feldspars also show evidence of framework grain dissolution (FGD), where the grain is leached and the dissolved components are completely removed from the immediate pore space (after Siebert et al, 1984; Moncure et al, 1984).

Plagioclase grains show the most FGA and frequently show preferential leaching along cleavage planes (Figures 30 and 31). Orthoclase feldspar grains are rarely dissolved but show signs of FGA, notably conversion to sericite or illite.

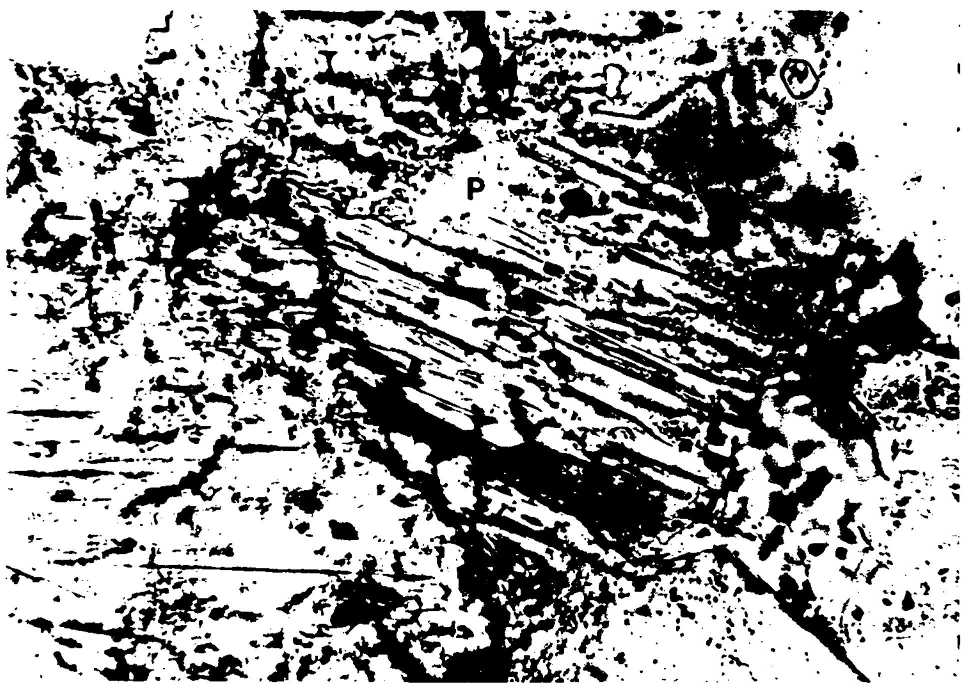

Figure 30: Plagioclase grain (P) showing preferential leaching along cleavage planes. The areas being replaced may be less stable due to higher Na content relative to the rest of the grain. Blue areas are pore space. Hardin 159' 6". plane light.

1.2 mm

Figure 31: Scanning electron micrograph showing evidence of preferential dissolution of feldspar along cleavage planes of plagioclase grain. Note formation of more resistant 'shelves' most likely caused by compositional differences within the grain. Hardin 159' 6", 4.0 Kv.

Frequently, orthoclase grains are not entirely altered, and it is apparent that clay crystals or sericite are aligned preferentially along cleavage planes. Wholesale FGA can be ubiquitous, most commonly seen as replacement of the feldspar grain by kaolinite. These altered grains often retain the original grain shape (Figures 12 and 18) and some of the authigenic clay replacements show evidence of compaction. Kaolinite is also frequently present as a pore filling in association with feldspar grains, and kaolinite always shows delicate crystalline morphologies, indicating an authigenic source (Figure 32). While complete feldspar grain alteration to sericite or illite is commonly observed in sandstone units, these clays are less abundant than kaolinite. However, the shales of the Ladore contain abundant illite, kaolinite and chlorite based on EDX data obtained from core samples.

Complete framework grain dissolution is not as common as framework grain alteration to clays in these sandstones, but when present can be easily recognized by large, over-sized pores which compose up to 14% of these sandstones. These oversized pores are often the same size and shape of adjacent sand-grains, and although no remnant of the original grain exists in most cases, they are assumed to be leached feldspar grains due to the extent of observable feldspar dissolution in these units (Figure 33).

Calcite cement is present as isolated patches in the coarser-grained sandstones, which show evidence of feldspar alteration. These patches of calcite cement are commonly adjacent to feldspars that have undergone partial dissolution, or are adjacent to feldspars that have been completely dissolved. Mechanisms for feldspar alteration have been proposed by Siebert et al. (1984) and Moncure et al. (1984) which attempt to explain how the dissolution of

1.0 mm

Figure 32: Scanning electron micrograph of kaolinite books. The delicate morphology of these clay crystals indicates authigenic origin. Hardin 159' 6", 5 Kv.

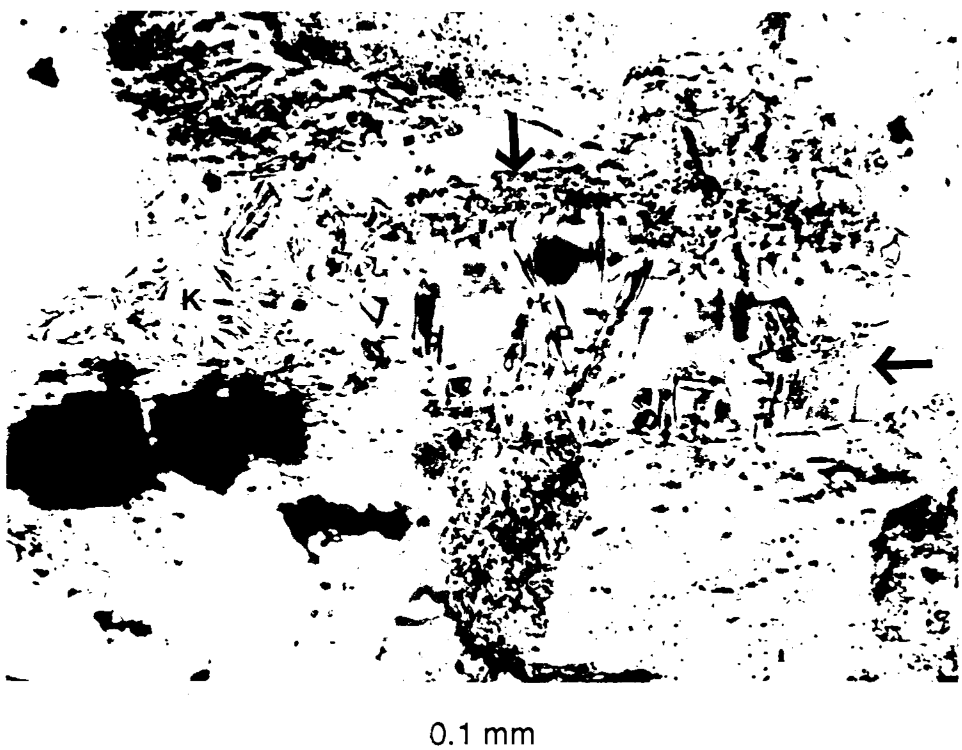

Figure 33: Feldspar grain, most likely plagioclase, showing extreme dissolution and generation of secondary porosity. The more stable cleavage planes (P) and outline of the grain can still be seen (arrows). Note kaolinite crystals (K) present in pore space. Hardin 159' 6", plane light.

feldspar takes place while calcite cement in the sandstone is preserved. This mechanism involves the conversion of smectite to illite in the shales surrounding these sandstones, which causes the removal of Al^{+3} from the shale water during clay diagenesis. As diagenesis proceeds, waters in the shale become increasingly acidic due to the addition of CO_2 released by maturation of organic matter present in the shale. These shale-waters are then expelled into the surrounding sandstone during compaction, where they act as solvents.

The disequilibrium with respect to aluminum of these solvents allow feldspars to be dissolved by interstitial fluids, according to the following reaction (from Siebert et al., 1984):

$$NaAlSi_3O_8 \text{ (albite)} + 2Ca^{+2}(aq) + 4HCO_3^-(aq) \dashrightarrow Na^+(aq) + Al(OH)_2^+$$

$$2HCO_3^- + 3SiO_2(s) \text{ (quartz)} + 2CaCO_3(s) \text{ (calcite)}$$

During this reaction calcite is precipitated as a cement, while feldspars are dissolved. This is consistent with the patchy occurrence of calcite observed in the sandstones of the Ladore Shale, in that they are in close proximity to feldspar-shaped secondary pores and partially dissolved feldspar grains.

In addition, the above reaction can explain the formation of over-sized pores and the partial dissolution of grains in the sandstones of the Ladore Shale. These secondary pores may be the voids remaining after Na-rich feldspars or albitized areas within feldspars adjacent to cleavage planes were dissolved by shale-water solvent. More stable feldspars such as potassium-rich orthoclase were not completely dissolved but instead appear to have been altered to clays such as kaolinite or illite, as described in the quartz cement section above.

The extent of FGA and FGD by shale-water solvents depends on three factors: 1) the amount of and type of organic material present in the shale, 2) the sand-to-shale ratio, and 3) the porosity of the sandstones that are being effected (Siebert et al., 1984). In general the shales of the Ladore are organic rich, mostly in the form of abundant plant material. The CO_2 produced during the oxidation of this plant material is the the most likely source of acid for in this reaction (Potter et al., 1980). Sand-to-shale ratios vary for each site, but the volume of shale is consistently large enough (greater than 1:10 sand to shale ratio) to supply the necessary CO_2 to drive this reaction (Siebert et al., 1984). As for porosity, feldspars in the coarse-grained sandstone lithofaces show more FGA and FGD compared to siltstones in the finer-grained lithofacies, which have fresh, unaltered feldspars. Finer-grained siltstone and sandstone lithologies are most commonly surrounded by low-permeability shale, which can be several feet (<2 m) thick. In addition, siltstone beds are often completely cemented with calcite cements that fill all available pore space. These two factors may have prevented chemically-active fluids from altering feldspars (and other grains) of the clay-shale and siltstone-shale lithofacies.

Pyrite

In the sandstones and siltstones of the Ladore Shale authigenic pyrite is seen as a replacement of organic material or calcite in shell fragments (Figure 34). Pyrite is present in the clay-shale lithofacies from core samples, occurring as isolated crystals, but was observed only in trace amounts in outcrop samples. Pyrite often forms in association with decaying organic material, where bacterial

Figure 34: Pyrite in micrite layer. Pyrite (P) replacing pink stained calcite (C) formed due to presence of organics in skeletal debris. Gaddy 307' 3", plane light.

reduction of organic sulfur is converted to FeS (know as hydrotroilite or mackinawite) (Pettijohn et al., 1987). During early diagenesis under locally reducing conditions caused by an abundance of detrital organic material, FeS can be converted to pyrite (Berner, 1980). The sulfur required for pyrite formation may have been released during the fixation as SO^{-4} present in formation water was reduced to S^{-} by bacteria during the oxidization of organic material. Iron may have entered the system from the leaching of iron rich minerals, such as ferroan carbonates or clays, or may have been present as Fe^{+2} ions dissolved in low-oxygen waters.

Paragenesis

Examination of grain and cement relationships in the sandstones, siltstones and shales of the Ladore suggest the following interpretation of the diagenetic sequence for these units:

Diagenetic sequence

The rock units of the Ladore shale have passed through several diagenetic regimes, each with particular conditions of pore-water chemistry, compaction, temperatures and mineral alteration. The transitions between regimes are not sudden, and represent the gradual changing subsurface conditions. The proposed paragenetic sequence is illustrated in figure 35.

Fresh water meteoric regime: The first stage of diagenesis most likely occurred in the meteoric phreatic regime, after minor compaction when these units were affected by fresh waters of the fluvial groundwater system. Soon after sediment transport and subsequent deposition, unstable mineral components such as feldspars were altered by the acidic nature of the meteoric waters.

Figure 35: Proposed paragenetic sequence for the Ladore Shale. Solid lines represent timing of diagenetic events, dashed lines represent time when diagenetic effects may not have been active. Stippled pattern represents gradational transition between diagenetic regimes.

[redacted]

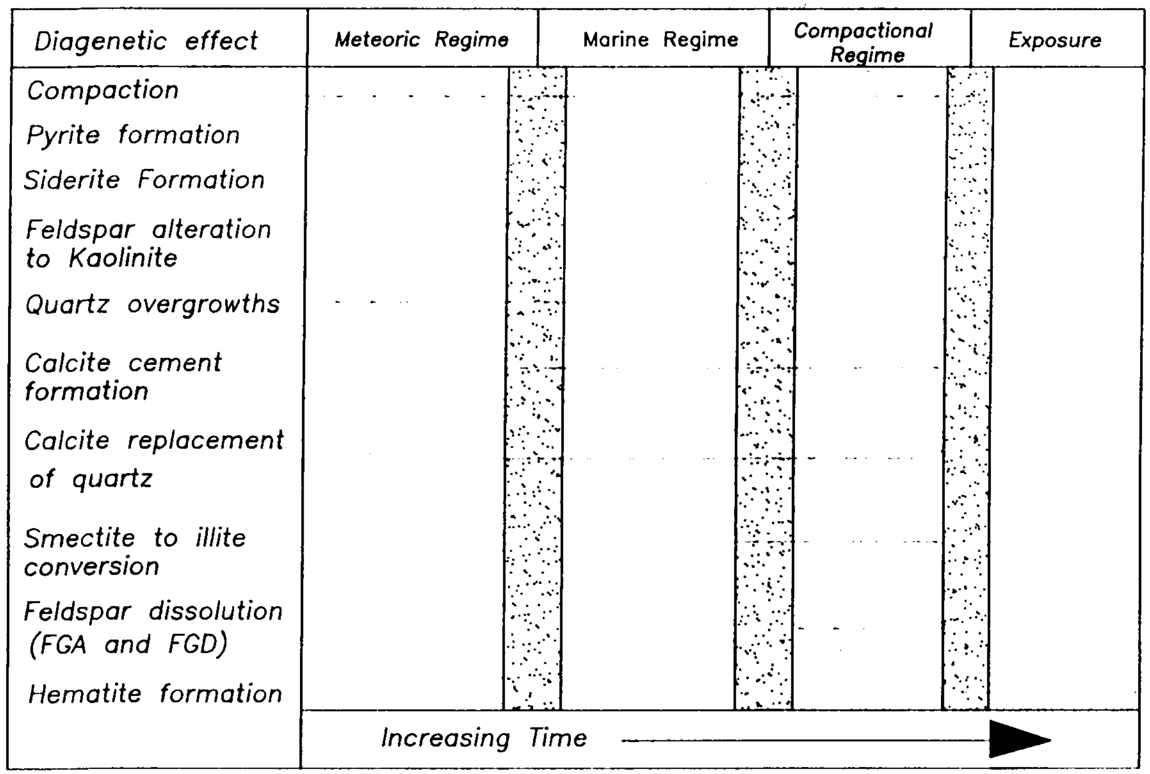

Diagenetic effect
Meteoric Regime
Marine Regime
Compactional Regime
Exposure
Compaction
Pyrite formation
Siderite Formation
Feldspar alteration to Kaolinite
Quartz overgrowths
Calcite cement formation
Calcite replacement of quartz
Smectite to illite conversion
Feldspar dissolution (FGA and FGD)
Hematite formation
Increasing Time

Alteration of potassium feldspars to clay occurred after deposition. Evidence for this is seen in partial alteration of feldspar grains to kaolinite, and the presence of dust rims of cly around detritial grains.

The beginning of the Mound Valley transgression decreased the influence of acidic fluvial waters which caused an increased in the pH of the interstitial water of these units. Silica liberated by the conversion of potassium feldspar to kaolinite was dissolved in pore-fluids of the sandstones and the relatively high porosity of these sandstones allowed unrestricted circulation of fluids through sandstone units. This circulation of fluid oversaturated with respect to silica precipitated syntaxial quartz-overgrowths on detrital quartz grains. These silica cements occur over clay dust rims, which represent the clays derived from feldspar alteration.

Marine regime: The next stage of diagenesis occurred after the transgression that deposited the Mound Valley Limestone occurred, and allowed more alkaline waters (pH around 8 and slightly oversaturated with carbonate) to replace meteoric waters in the pore space of these units. During this transgression only minimal compaction occurred (due to the deposition of only a relatively thin layer of limestone) and poikilitopic calcite cement was precipitated. The slight oversaturation of calcite in these waters allowed slow formation of large crystals of calcite around limited nucleation points (most likely carbonate grains). In addition, these waters were oxygen depleted due to the ongoing oxidization of buried organic matter, thereby allowing dissolved iron to be incorporated into the calcite cements. Replacement of quartz by calcite most likely occurred contemporaneous with the deposition of the calcite cements, as evidenced by grain-edge embayment of the detrital quartz grains.

Grain-to-grain contacts and deformed mineral grains, particularly micas, indicate that mild compaction occurred in most sandstones before calcite cement was fully precipitated, some time after these units were deposited.

Organic material was replaced by pyrite about the same time as these units were affected by marine waters. The oxidization of organic material may have reduced the amount of dissolved oxygen in pore-fluids allowing anaerobic decay to commence. Bacterial action resulted in S^{-2} production from SO^{-4} present in seawater and this combined with dissolved iron, forming pyrite in association with organic material.

Compactional regime: The third major phase of diagenesis occurred after the main phase of poikilotopic calcite cement precipitation, when compaction due to the increasing weight of overlying sediments (most likely the deposition of the Galesburg Shale and overlying units) may have significantly decreased original porosity in units which were not tightly cemented. Clay shales and non-cemented siltstones were the units most affected by lithostatic pressure. This compaction was not great enough however, to cause suturing of detrital mineral grain boundaries. Siderite nodules most likely formed early soon after deposition in oxygen poor environment before marine waters entered the system, although these nodules were later effected by compaction as suggested by their flattened-disc morphology.

Due to increased depth in the sediment pile (and a slight geothermal gradient), temperature was elevated to >50° C, and soon after, the conversion of smectite to illite occurred in the shale units. This clay mineral transformation is thought to occur in the compactional regime, where temperatures and pressures were increasing due to the growing height of sediment above. During the alteration of smectite to illite, the shale-waters became depleted with respect to Al^{+3}, while additional CO_2 production from the decay of organic matter lowered the pH. The maturation of clays and organics in the shale produced a shale-water solvent capable of dissolving feldspar grains. These acidic, Al^- depleted waters were expelled from the shales, possibly pushed out by lithostatic pressure or due to CO_2 production, and effected the nearby sandstone units causing the partial or complete dissolution of Na-rich feldspars grains or Na-rich zones within grains. These alterations produced the fabric of framework grain alteration and framework grain dissolution, which increased secondary porosity in these units.

Most likely, calcite cement in the sandstones was partially leached prior to the dissolution of feldspars, thereby increasing secondary porosity and permeability in the sandstone units and allowed shale water solvent access to these units. Whatever the exact timing of the partial dissolution of the cement, finer-grained siltstones and sandstones which were surrounded by low-permeability shales were not affected by these solvents and often contain fresh, unaltered feldspar grains.

The major compaction episode is particularly noticeable in the finer-grained siltstones and sandstones, which exhibit a tightly packed grain fabric and are cemented with pore-filling cement. This later cement may have resulted from the release of carbonate into pore-fluids during the smectite to illite transformation. In addition, calcite replacement of these tightly-packed quartz grains occurred also by the thin-film process contemporaneous to carbonate deposition.

Exposure : After exhumation and modern exposure, oxygen rich meteoric water in the vadose zone effected these units. Ferroan calcite was dissolved, releasing Fe^{+3}, which in oxygen-rich waters formed hematite. The "box-work" structures, which are common in outcrop, formed as ferroan calcite was dissolved and hematite precipitation was concentrated on calcite cleavage planes.

CONCLUSIONS

Based on sedimentologic and petrographic analyses of the cores and outcrops of the Ladore Shale, including microanalyses of thin sections and the construction of a cross-section and isopach map for this unit, the following conclusions can be drawn about the petrology, depositional and diagenetic environments of the Ladore Shale:

The three lithofacies recognized for this unit were deposited as elements of a delta system that prograded across the Cherokee shelf. The silty-clay shale lithofacies was predominantly deposited in a prodeltaic to delta-front environment, although this lithofacies represents several different depositional facies. Thin marine carbonate horizons indicate delta-lobe switching may have temporally cut off terrestrial sediment input to the to the immediate area, thus causing local marine transgression. Thin coal beds occur in this lithofacies, which indicate sub-aerial exposure, possibly upon a crevasse-splay or bay-fill facies. The siltstone-shale lithofaces represent distal bar and distributary bar facies, which were deposited seaward of the distributary channel discharge. The sandstone lithofacies represents deposition in distributary channels within the lower delta plain. All of these environments may have been affected by tidal processes and reworking of sediments.

The highly lobate form of the sediments of the Ladore Shale, as illustrated in the isopach map for this unit, indicates that this delta system was dominated by river sedimentation processes and was not significantly effected by waves or longshore currents and processes.

Depositional source direction inferred from the isopach map of this unit suggests that the paleosource was to the south-southeast. The sediments that form the Ladore Shale were probably derived from the Ouachita mountains, which were the dominant positive topographic feature that contributed detritus to this area during the Missourian.

Diagenesis began effecting the rocks of the Ladore Shale soon after deposition as siderite nodules formed after oxygen was depleted, but before much compaction occurred or sulfur became available. Feldspar grains were altered to kaolinite by slightly acidic fluvial waters present during deposition. The silica released by this reaction initiated the formation of quartz overgrowths in the siltstones and sandstones that had sufficient porosity and permeability to transmit fluid.

After the succeeding transgression began depositing the overlying Mound Valley Limestone, interstitial waters became effected by marine waters, oversaturated with respect to $CaCO_3$, and poikilotopic calcite cement was precipitated. Continued reduced oxygen conditions in these waters allowed Fe-rich calcite to form, and an increase in sulfur from SO^{-4} in the marine water allowed pyrite to form as well.

Later during the Missourian, the Galesburg Shale was deposited during a regressive event, and the weight of these and subsequently deposited sediments increased compaction due to deeper burial of the Ladore Shale units. The increased temperatures at depth initiated the conversion of smectite to illite in the shale-rich portions of the Ladore. This conversion formed a shale-water solvent, that was able to alter the feldspars in the sandstones and siltstones of the Ladore. Late stage pore-filling calcite cement was a by product of this reaction. After modern exposure at the surface, iron-rich calcite was dissolved, thereby liberating Fe^{+3}, which formed the hematite cements that are conspicuous in outcrops of the sandstones in Ladore Shale.

REFERENCES

Adams, G. I., 1904. Gypsum Deposits of America, U.S. Geologic Survey Bull. 223, p. 1-73.

Berner, R. A. 1980. Early Diagenesis, Princeton University Press, Princeton, NJ, p. 241.

Bjørlykke, K, 1984. Formation of Secondary Porosity: How important is it?, in McDonald, D. A., and Surdam, R. C. (eds.), Clastic Diagenesis, American Association Petroleum Geologists, Memoir 37, p. 217-224.

Bjørlykke, K, 1988. Sandstone diagenesis in relation to preservation, destruction and creation of porosity, in Chilingarian, C. V., and Wolf, K. H. (eds.), Diagenesis. I, Developments in Sedimentology 41, Elsevier, Amsterdam, 591 PSG.

Blatt, H. 1979. Diagenetic Processes in Sandstones, in Aspects of Diagenesis, SEPM special publication 26, p. 141-157.

Boardman, D. L. and Heckel, P. H. 1989. Glacial eustatic sea level curve for early Late Pennsylvanian sequence in north-central Texas and biostraigraphic correlation with curve for Midcontinent North America. Geology, v.17, p.802-805.

Boles, J. R., 1984. Secondary porosity reactions in the Stevens Sandstone, San Joaquin Valley, California, in McDonald, D. A., and Surdam, R. C. (eds.), Clastic Diagenesis, American Association Petroleum Geologists, Memoir 37, p. 217-224.

Boles, J. R., and Franks, S. G., 1979. Clay diagenesis in Wilcox sandstones of southwest Texas: implications of smectite diagenesis on sandstone cementation. Journal Sedimentary Petrology, v. 49, p. 55-70.

Brenner, R. L., Ludvicson, G. A., Scal, R., and Dogan, A. U., 1991. Diagenetic Modeling of Siliciclastic Systems: Status Report, in Franceen, E. K., Watney, W. L., Kendall, C. G. S. C., and Ross, W. (eds.), Sedimentary Modeling, Computer Simulations and methods for Improved Parameter Definition. K.G.S. Bull., v. 233, p. 123-137.

Burley, S. D. and Kantorowicz, J. D. 1986. Thin section and S.E.M. textural criteria for the recognition of cement-dissolution porosity in sandstones, Sedimentology, v. 33, p. 587-604.

Coleman, J. M. and Gagliano, S. M. 1965. Sedimentary Structures: Mississippi River Deltaic Plain, in Middleton, G. V. (ed), Primary Sedimentary Structures and their Hydrodynamic Interpretation, SEPM Special Publication 12, p. 133-148.

Coleman, J. M. and Prior, D. B. 1982. Deltaic Environments of Deposition, in Horn, M. K. (ed.), Sandstone Depostional Environments, American Association Petroleum Geologists, Memoir 31, p. 139-179.

Dapples, E. C., 1971. Physical classification of carbonate cement in quartzose sandstones. Journal of Sedimentary Petrology, v. 41, p. 196-204.

Fisher, W. L., Brown, L. F. et. al., 1969. Delta systems in the exploration for oil and gas, Bureau of Economic Geology, Univ. of Texas, Austin, p. 77.

Galloway, W. E., 1984. Hydrogeologic regimes of sandstone diagenesis, in McDonald, D. A., and Surdam, R. C. (eds.), Clastic Diagenesis, American Association Petroleum Geologists, Memoir 37, p. 3-13.

Heckel, P. H. 1972. Recognition of Ancient Shallow Marine Environments, in Rigby, J. K. and Hamblin, W. K., (eds.), Recognition of Ancient Sedimentary Environments, SEPM Special Publication No. 16, p. 215-286.

Heckel, P. H. 1977. Origin of phosphatic black shale Facies in Pennsylvanian Cyclothems of Mid-Continent North America, AAPG Bull., v. 61, no. 7, p. 1045-1068.

Heckel, P. H. 1980. Paleogeography of eustatic model for deposition of Midcontient Upper Pennsylvanian cyclothems: in Fouch, T. D. and Magathan, E. R., eds., Paleozoic Paleogeography of the West-Central United States: Rocky Mountain Section, Society of Economic Paleontologists and Mineralogists, Rocky Mountain Paleogeography Symposium 1, p. 196-216

Heckel, P. H., 1983. Diagenetic model for carbonate rocks in Midcontinent Pennsylvanian eustatic cyclothems. Journal Sedimentary Petrology, v. 53, p. 733-759.

Heckel, P. H., 1984, Changing concepts of midcontinent Pennsylvanian cyclothems, North America: Ninth International Carboniferous Congress, Compte Rendu, v. 3, pt. 3, Southern Illinois University, Carbondale, IL, p. 535-553.

Hinds, H., Greene, F. C. 1915. The stratigraphy of the Pennsylvanian series in Missouri. Missouri Bureau of Geology. and Mines, v. 3, p. 26

Hucheon, I., 1983. Aspects of the Diagenesis of Coarse Grained Siliciclastic Rock, Geoscience Canada, v. 10, p. 4-13.

Leder, F. and Park, W. C., 1986. Porosity reduction in sandstone by quartz overgrowth. American Association Petroleum Geologists, Bulletin, v. 70, p. 1713-1728.

Lindholm R. C. and Finkleman, R. B. 1971. Calcite Staining: Semiquantitative Determination of Ferrous Iron, Jour. of Sed. Pet., v.42, no. 1, p. 239-242.

Moncure, G. K., Lahann, R. W., and Siebert, R. M., 1984. Origin of secondary porosity and cement distribution in a sandstone/shale sequence from the Frio Formation (Oligiocene), in McDonald, D. A., and Surdam, R. C. (eds.), Clastic Diagenesis, American Association Petroleum Geologists, Memoir 37, p. 151-175.

Moore, R. C. 1936. Stratigraphic classification of the Pennsylvanian rocks of Kansas. Kansas Geological Survey, Bull. 22, p. 90

Pettijohn, F. G., Potter, P. E., and Siever, R., 1987. Sand and Sandstone, Second Edition. Springer-Verlag, New York, 553 p.

Potter, P. E., Maynard, J. B. and Prior, W. A. 1980. Sedimentology of Shale, First Edition. Springer-Verlag, New York, p. 309.

Rascoe, B., Adler, F. J. 1983. Permo-Carboniferous hydrocarbon accumulations, midcontinent, U.S.A. American Association of Petroleum Geologists, Bull., v. 67, p. 979-1001.

Siebert, R. M., Moncure. G. K. and Lahann, R. W., 1984. A Theory of Framework Grain Dissolution in Sandstones, in McDonald, D. A., and Surdam, R. C. (eds.), Clastic Diagenesis, American Association Petroleum Geologists, Memoir 37, p. 163-175.

Surdam, R. C., Boese, S. W., and Crossey, L. J., 1984. The chemistry of secondary porosity, in McDonald, D. A., and Surdam, R. C. (eds.), Clastic Diagenesis, American Association Petroleum Geologists, Memoir 37, p. 127-150.

Swanson, D. C. 1979. Deltaic Deposits in the Pennsylvanian Upper Morrow Formation of the Anadarko Basin, in Hyne, N. J. (ed.), Pennsylvanian Sandstones of the Mid-Continent, Tulsa Geological Society Special Publication 1, p. 115-169.

Visher, G. S., Ekebafe, S. B and Rennison, J. 1980. The Coffeyville Format (Pennsylvanian) of Northern Oklahoma, A Model for a Epieric Sea Delta, in Broussard, M. L. (ed.), Deltas: Models for Exploration, Second Edition, Houston Geological Society, p. 555.

Watney, W. L., French, J. A., and Franceen, E. K. 1989. Sequence stratigraphy interpretations and modeling of cyclothems in the Upper Pennsylvanian (Missourian) Lansing and Kansas City Groups in eastern Kansas: Kansas Geologic Society Guidebook, 41st Annual Field Trip, 211 p.

APPENDIX A:
OUTCROP AND CORE DESCRIPTIONS

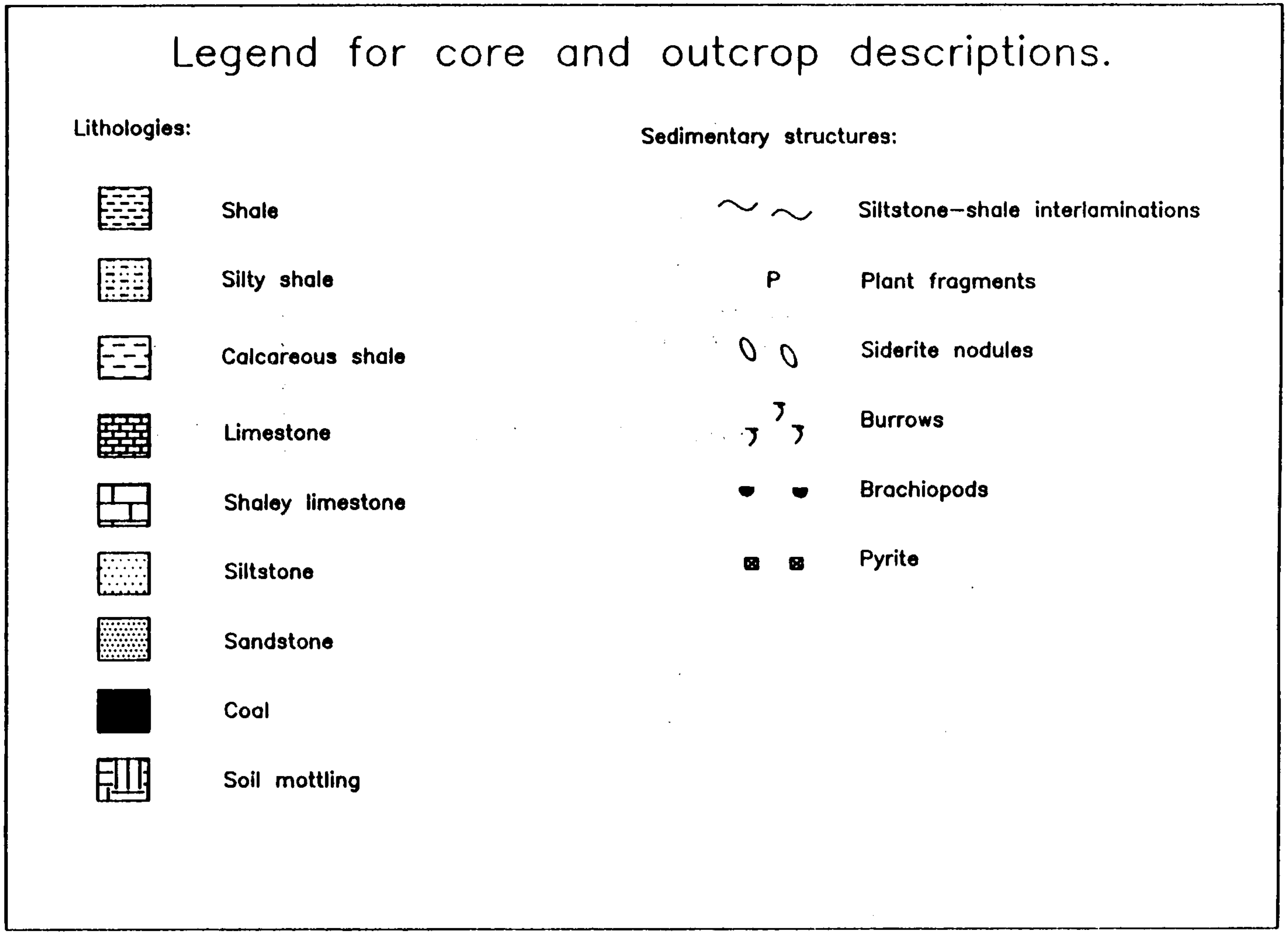

Legend for core and outcrop descriptions.

Section: Page's Pasture

State: Kansas

Location: SW/SW Sec. 31, T27S, R21E

County: Neosho

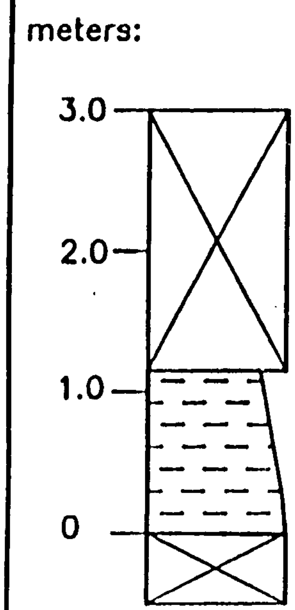

Ladore Shale

0 to 1.1 m
Grey shale, thinly bedded. Orange mottles common. Pore exposure, highly weathered.

Section: North Erie

State: Kansas

Location: NW Sec. 20, T28S, R20E

County: Neosho

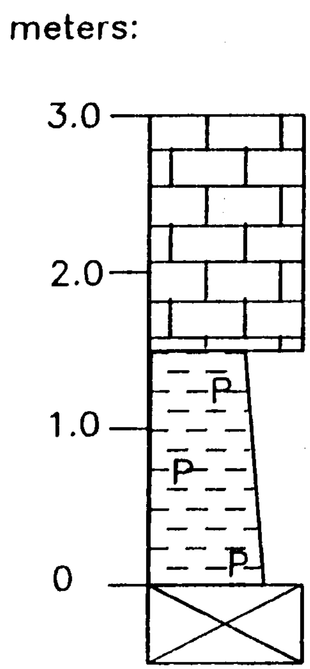

Mound Valley Limestone

1.5 to 3.0 m
Calculutite, crinoid and brachiopods common.

Ladore Shale

0 to 1.5 m
Grey, calcareous shale. Small plant fragments (<2cm) common. some mottling in upper 10 cm.
Covered lower contact.

[redacted]

Section: South Erie

State: Kansas

Location: NW/NW Sec. 7, T29S, R20E

County: Neosho

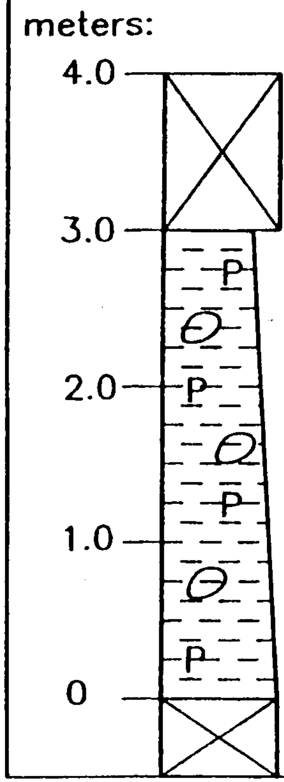

Ladore Shale

0 to 3.0 m
Grey, clay shale. Siderite nodules common below 2.0m, rare above. Small plant fragments common, decreasing upwards. Orange mottling at top of outcrop.
Covered upper and lower contacts.

Section: Parsons Lake (Type Ladore)
Location: NW/NW/NE Sec. 33, T30S, R19E

State: Kansas
County: Neosho

meters: samples:

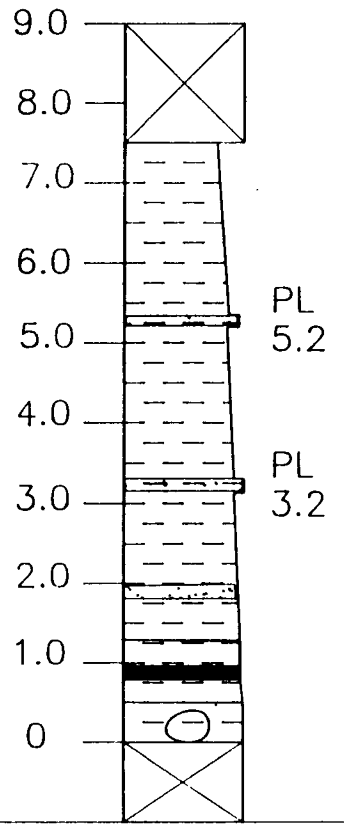

Ladore Shale

0.7 to 7.4 m
Clay shale with thin (<2cm) calcite cemented siltstone beds and thin calcilutite beds common. Siltstone beds continuos for width of outcrop, > 20m. Siltstone beds may have wavy laminations and burrows. Abrupt lower contact.

0.5 to 0.7 m
Thin (.1m) coal bed underlain by .1m thick grey shale underclay.
Abrupt lower contact.

0 to 0.5 m
Thin bedded silty clay shale, abundandt large plant fragments up to .5m long. Siderite nodules common.
Covered lower contact .

Section: Dixon Mound
Location: SE/SE Sec. 27, T32S, R18E

State: Kansas
County: Labette

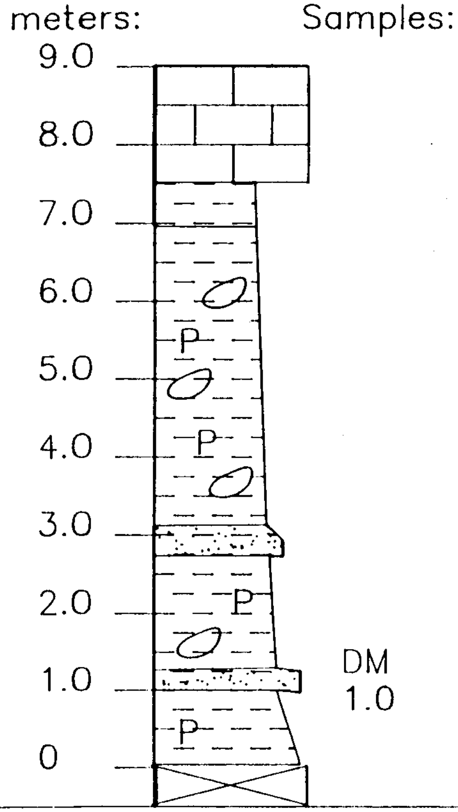

Mound Valley Limestone

7.5 to 9.0 m
Dense, grey calcilutite. Fossils rare.

Ladore Shale

7.0 to 7.5 m
Grey/orange mottles, shale chips and altered plant fragments. Decreasing alteration downward.

0 to 7.0 m
Fissile grey to black clay shale.
Abundant large plant fragments and siderite nodules (<5cm). Thin siltstone beds (<2cm) occasional, absent above 3.5 m.

Section: Big Hill

State: Kansas

Location: SW/SE, Sec 27, T32S, R19E

County: Labette

meters: Sample:

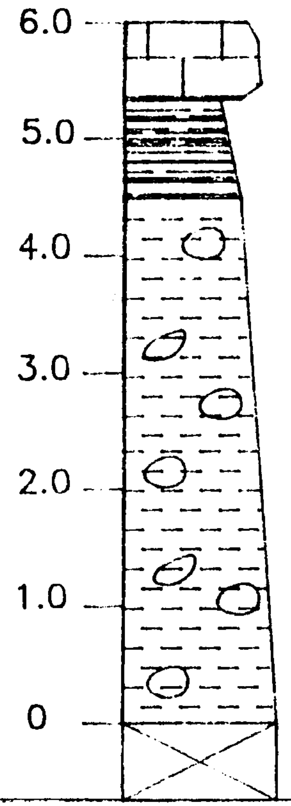

BHL
1.6

Mound Valley Limestone

5.4 to 6.0 m
Calcilutite, abundant large crinoid pieces. Massive bedding.

Ladore Shale

4.5 to 5.4 m
Orange/grey mottled clay shale. Plant fragments common, siderite nodules rare.

0 to 4.5 m
Thin bedded clay shale, abundant plant fragments, thin silty zones common. Siderite nodules abundant, some >5cm. Occasional large plant fragments, >30cm and 3 cm thick.

Section: Sapulpa Shale Pit

State: Oklahoma

Location: SW/NW Sec. 34, T18N, R11E

County: Creek

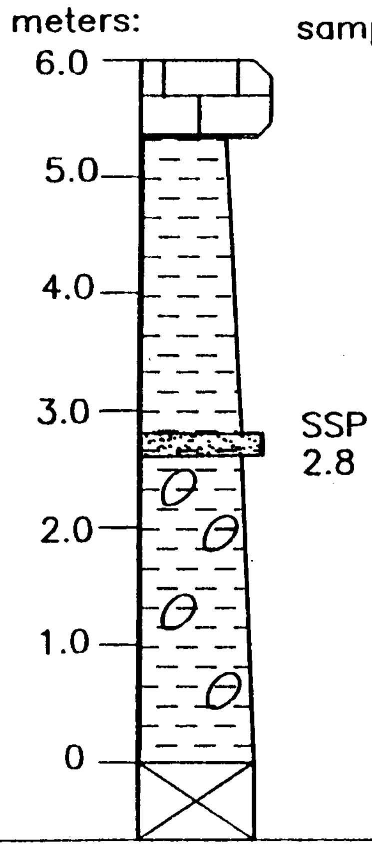

Mound Valley Limestone

5.1 to 6.0 m
Crinoidal limestone, very well indurated
Sharp lower contact.

Ladore Shale

0 to 5.1 m
Grey shale, siderite nodules common below 3.0m.
Fine siltstone layer at 2.8m, 5cm thick.
Lower contact covered.

Section: Lower Coffeyville

State; Oklahoma

Location: NE/SE Sec. 14, T20N, R13E

County: Tulsa

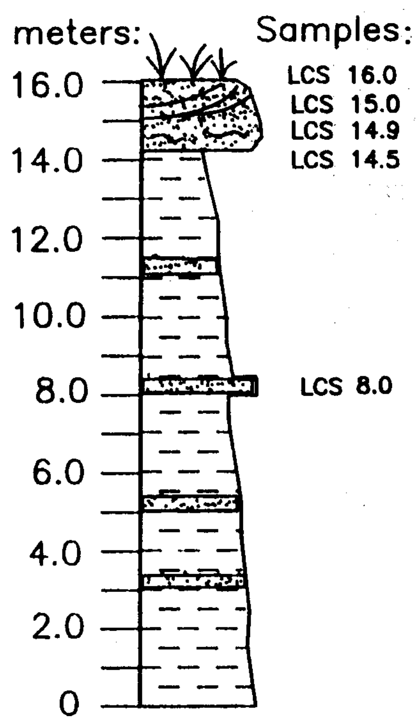

Ladore Shale

14.8 to 16 m
Sandstone, massive beds, occasional trough crossbed sets with 8 to 10 cm wavelength, < 2 cm amplitude. Plant fragments rare. Brown stained.

14.3 to 14.8 m
Lenticular and wavy siltstone interlaminations with shale. Some herringbone interlaminations and small ripples (<3 cm). Abrupt lower contact.

0 to 14.3 m
Thin bedded shale with occasional thin siltstone beds (<10 cm thick). Siderite nodules common, plant fragments absent.

Core: K.G.S. Dotson Interval: 69' 0" to 73' 0", 21.2 to 21.9m

Unit Number	Depth (ft)	Lithology	Sample Location	Core Descriptions	Interpretations
3	69'	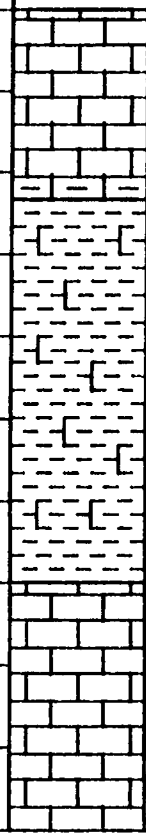		Unit 3: 69'8" + <21.2 m Oolitic limestone with extreme grain dissolution. Oil shows. Grain size decreasing down, to arg. limestone at base.	Mound Valley Limestone.
2	70' 71'			Unit 2: 72' 0" to 69' 8" 21.9 to 21.2 m Silty calcareous shale, decreasingly calcareous upwards. Abrupt basal contact.	Ladore Shale.
1	72' 73'			Unit 1: >72' 0" >21.9 m Calcilutite, with increasing skelital grains downward.	Bethany Falls Limestone.

Core: K.G.S. Hines   Interval: 128' to 113', 39.0 to 34.4 m

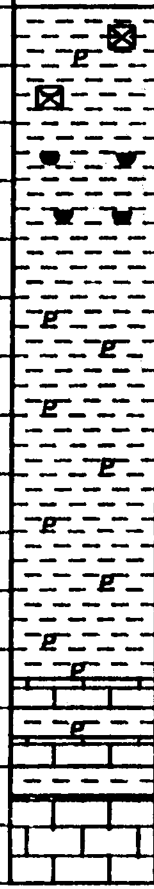

Unit Number	Depth (ft)	Lithology	Sample Location	Core Descriptions	Interpretations
4	114, 116			Unit 4: 118' 0" to 110' 6" 35.9 to 33.7 m Shale with calcareous shelly layers common. Large brachiopods common, pyrite common above 115', rare below. Frequent small shelly zones, some occasional small plant fragments. Gradational contact.	
3	118, 120, 122			Unit 3: 124' 0" to 118' 0" 37.8 to 35.9 m Finely lamanated silty shale with abundant plant fragments which decrease in size and abundance upwards. Gradational lower contact.	Ladore Shale.
2	124			Unit 2: 126' 3" to 124' 0" 38.5 to 37.8 m Silty shale with abundant large plant fragments, calcareous shell layers. Brown oxidization layers common, decreasing upwards. Abrupt lower con.	
1	126			Unit 1: >126' 3" >38.5 m Arg. limestone, abundant shell fragments.	Bethany Falls limestone.

Core: K.G.S. Hines   Interval: 113' to 108', 34.4 to 32.6 m

Unit Number	Depth (ft)	Lithology	Sample Location	Core Descriptions	Interpretations
	108'	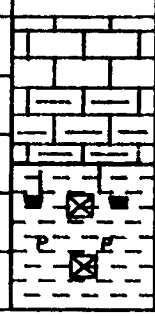			
5	110'			Unit 5: 110' 0" to 109' 0" 33.7 to 33.2 m Arg. limestone containing brachiopods and crinoid pieces. Increasingly calcareous upwards grading into calcilutite. Gradational lower contact.	Bottom of Mound Valley limestone.
4	112'				

Core: K.G.S. Heilman   Interval: 145' to 130', 44.2 to 39.6 m

Unit Number	Depth (ft)	Lithology	Sample Location	Core Descriptions	Interpretations
3				Unit 3: 131' 4" to 128' 0" 40.0 to 39.0 m Calcareous silty shale with interlaminated silt beds and occasional burrows. At top unit grades into arg. limestone. Plant fragments decrease in abundance above 128' 6". Brown halos common. Gradational lower contact.	
2	132' 134' 136' 138' 140' 142'	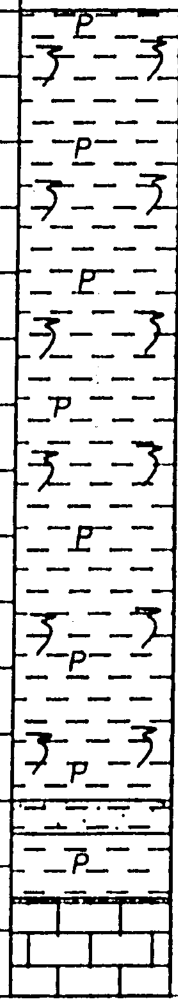	Heil 140'9"	Unit 2: 143' 7" to 131' 4" 43.7 to 40.0 m Silty shale with thin calcareous silt interlaminations. Abundant burrows filled with calcareous silt. Large plant fragments abundant, occasional brown halos, some silt laminations show cross-bedding. Increasingly calcareous towards top. Gradational lower contact.	Ladore shale. Very uniform above 142', more silt lam. below 142'.
1	144'			Unit 1: >143' 7" >43.7 m Limestone, abruptly gradational upper contact. Thin calcareous shale at top.	Bethany Falls limestone.

Core: K.G.S. Heilman   Interval: 145' to 130', 44.2 to 39.6 m

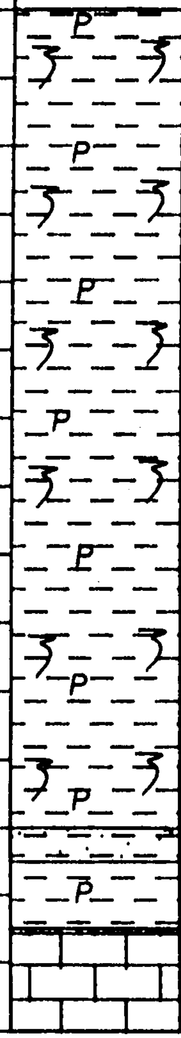

Unit Number	Depth (ft)	Lithology	Sample Location	Core Descriptions	Interpretations
3				Unit 3: 131' 4" to 128' 0" 40.0 to 39.0 m Calcareous silty shale with interlaminated silt beds and occasional burrows. At top unit grades into arg. limestone. Plant fragments decrease in abundance above 128' 6". Brown halos common. Gradational lower contact.	
2	132' 134' 136' 138' 140' 142'		Heil 140'9"	Unit 2: 143' 7" to 131' 4" 43.7 to 40.0 m Silty shale with thin calcareous silt interlaminations. Abundant burrows filled with calcareous silt. Large plant fragments abundant, occasional brown halos, some silt laminations show cross-bedding. Increasingly calcareous towards top. Gradational lower contact.	Ladore shale. Very uniform above 142', more silt lam. below 142'.
1	144'			Unit 1: >143' 7" >43.7 m Limestone, abruptly gradational upper contact. Thin calcareous shale at top.	Bethany Falls limestone.

Core: K.G.S. Kinne Interval: 115' to 100', 35.1 to 30.5 m

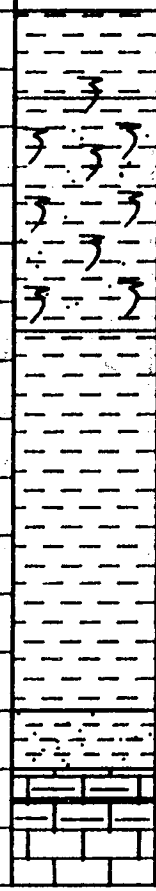

Unit Number	Depth (ft)	Lithology	Sample Location	Core Descriptions	Interpretations
5	102' 104'		Ki 105'4"	Unit 5: 105' 6" to101' 3" 32.2 to 30.8 m Shale with calcareous interlam. decreasing upwards. highly burrowed, abundant brown zones. Gradational lower contact.	Ladore Shale
4	106' 108' 110' 112'			Unit 4: 112' 5" to 105' 6" 34.3 to 32.2 m Clay shale, abundant brown zones, often parallel to bedding. Brachiopods rare. Grad.low. con.	
3				Unit 3: 113' 3" to 112' 5" 34.5 to 34.3 m Slightly silty shale, abundant plant fragments. Brown zones and burrows absent. Silt decreasing upwards. Gradational lower contact.	
2	114'		Ki 113'4"	Unit 2: 113' 6" to 113' 3" 34.6 to 34.5 m Arg. limestone/limey shale with abundant skeletal debris. Abrupt lower contact.	
1				Unit 1: 115' 6" to 113' 6" 35,2 to 34.6 m Calcarenite grading upwards into calcilutite.	Bethany Falls limestone.

Core: K.G.S. Kinne   Interval: 100' to 85', 30.5 to 25.9 m

Unit Number	Depth (ft)	Lithology	Sample Location	Core Descriptions	Interpretations
8	86' 88'			Unit 8: 90' 0" to 79' 6" 27.4 to 24.2 m Clay shale, rare small bivalves, increasing upwards. Abundant brown zones below 83'. Gradational lower contact.	Small halos around plant fragments or burrows.
7	90' 92' 94'	P		Unit 7: 97' 0" to 90' 0" 29.6 to 27.4 m Clay shale, large plant fragments abundant, size and abundance increasing upwards. Brown zones abundant. Gradational lower contact.	Shale lam. not disrupted by brown color zones.
6	96' 98'			Unit 6: 101' 3" to 97' 0" 30.8 to 29.6 m Clay shale, abundant brown zones. Plant fragments and burrows absent. Gradational lower contact.	

Core: K.G.S. Kinne   Interval: 84' to 78', 25.9 to 21.3 m

Unit Number	Depth (ft)	Lithology	Sample Location	Core Descriptions	Interpretations
9	76' 78'	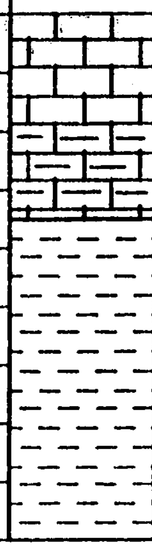		Unit 9: <79' 6" <24.2 m Arg. limestone grading into calcarenite. Contains large brachiopods and crinoid fragments.	Gradational contact between Ladore and Mound Valley between 80' and 78'.
8	80' 82' 84'				

Core: K.G.S. Newland Interval: 199' to 197'; 60.7 to 59.2 m

Unit Number	Depth (ft)	Lithology	Sample Location	Core Descriptions	Interpretations
3	197' 197'6"			Unit 3: <197' 11" <60.3 m Calcilutite with abundant small brachiopod, crinoid and fossil debris. Abrupt lower cont.	Mound Valley Limestone.
2	198' 198'6"			Unit 2: 198' 9" to 197' 11" 60.6 to 60.3 m Slightly silty shale with abundant small shell debris, increasing upwards. Abrupt lower contact.	Feather edge of Ladore Shale.
1	199'			Unit 1: > 198' 9" >60.6 m Oolitic limestone.	Bethany Falls Limestone.

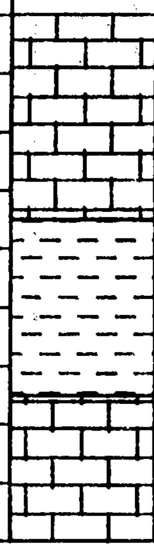

Core: K.G.S. Loflin   Interval: 171' 3" to 167' 6", 52.1 to 51.2 m

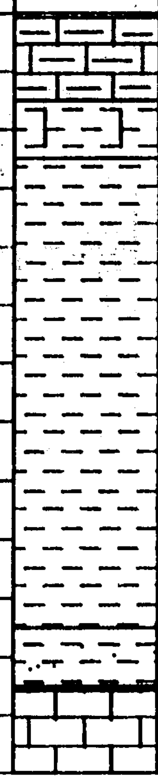

Unit Number	Depth (ft)	Lithology	Sample Location	Core Descriptions	Interpretations
5				Unit 5: <168' 3" <52.3 m Arg. limestone grading up into calcilutite. Abundant shell debris. Grad. lower contact.	Mound Valley limestone.
4	168'			Unit 4: 168' 5" to 168' 3" 51.4 to 52.3 m Calcareous silty shale. Increasingly calcareous upwards occasional brachiopods and fine shell debris. Gradational lower contact.	
3	168'6", 169', 169'6", 170'			Unit 3: 170' 6" to 168' 5" 51.9 to 51.4 m Silty shale, occasional brown halos. Sharp lower contact.	Ladore Shale.
2				Unit 2: 170' 9" to 170' 5" 52.1 to 52.9 m Silty shale, abundant bivalve fragments. Abrupt lower contact.	
1	170'6"			Unit 1: >170' 9" >52.1 m Calcilutite, fossils rare.	Bethany Falls limestone.

[redacted]

Core: K.G.S. Gaddy   Interval: 304' to 319', 94.3 to 97.1 m

Unit Number	Depth (ft)	Lithology	Sample Location	Core Descriptions	Interpretations

Unit Number: 10, 9, 8, 7, 6, 5, 4, 3, 2, 1

Depth (ft): 306', 308', 310', 312', 314', 316', 318'

Lithology:

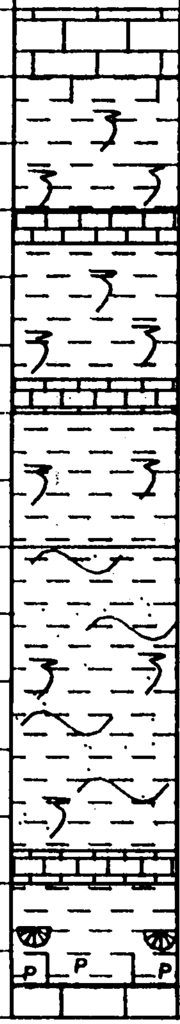

Sample Location:
G 307'3"s
G 309'11"
G 313'6"
G 314'2"
G 315'4"
G 315'4"s
G 316'4"
G 316'8"
G 317'3"

Core Descriptions:

Unit 10: 304' 8"+, 94.3+ m
Limestone, brachiopods common.
Sharp lower contact.

Unit 9: 309' 10" to 304' 8", 94.4 to 94.3 m
Shale, occasional burrows and interlaminations of calcareous silt. Increasingly fossiliferous upwards. Brachiopods and bryozoans present.
Sharp lower contact.

Unit 8: 310' 2" to 309' 10", 95.1 to 94.4 m
Thin calcarenite, some mud filled burrows.
Sharp lower contact.

Unit 7: 312' 0" to 310' 2", 95.0 to 95.1 m
Shale, occasional burrows filled with silt. Halos common. Abruptly gradational lower contact.

Unit 6: 316' 10" to 312' 0", 96.6 to 95.1 m
Shale with occasional siltstone interlaminations, frequent burrows filled with calcareous silt. Abruptly gradational lower contact.

Unit 5: 316' 7" to 314' 1", 95.7 to 96.6 m
Siltstone and shale interlaminations, some with cross-beds and truncations surfaces.
Occasional burrows. Abrupt lower contact.

Unit 4: 316' 10" to 316' 7", 96.6 to 96.7 m
Fine sandstone interlaminations with thin shale beds. Abrupt lower contact.

Unit 3: 318' 4" to 316' 10", 97.0 to 95.7 m
Grey shale, small brachiopods at base, bedding absent. Abrupt lower contact.

Unit 2: 318' 6" to 318' 4", 97.1 to 97.0 m
Fossiliferous calcareous shale. Abraided shell debris and large plant fragments common.
Abrupt lower contact.

Unit 1: <318' 6", <97.1 m
Limestone, brachiopods and shell debris common. Sharp upper contact.

Interpretations:

Mound Valley limestone.

Ladore Shale.

Numerous marine horizons present.

Bethany Falls limestone.

Core: K.G.S. Olson Interval: 373' to 358', 113.6 to 109.1 m

Unit Number	Depth (ft)	Sample Location	Core Descriptions	Interpretations
5	360', 362', 364'		Unit 5: 364' 6" to 348' 6" 111.1 to 106.2 m Micaceous shale, abundant brachiopods and plant debris increasing upwards. Few nodules and halos present. Gradational lower contact.	
4	366', 368'		Unit 4: 369' 6" to 364' 6" 112.6 to 111.1 m Silty shale, slightly calcareous, rare small brachiopods, nodules above 368' 6". Abrupt lower contact.	
3	370'		Unit 3: 369' 10" to 369' 6" 112.7 to 112.6 m Calcareous shale, small brachiopods abundant, scattered crinoid debris no laminations. Sharp low. con.	Bottom of Ladore shale.
2			Unit 2: 371' 4" to 369' 10" 113.2 to 112.7 m Calcilutite, brachipods common, upper contact abrupt. Sharp lower contact.	Thin Bethany Falls limestone
1	372'		Unit 1: >371' 4" >113.2 m Calcareous shale, fossil fragments common.	Hushpuckney shale.

[redacted] [redacted]

Core: K.G.S. Olson Interval: 358' to 343', 109.1 to 104.5 m

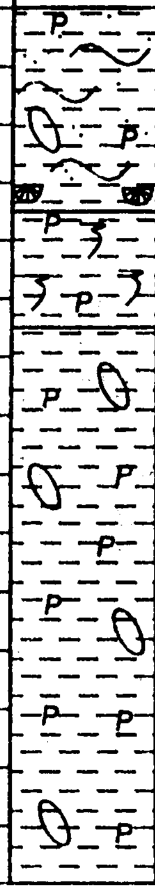

Unit Number	Depth (ft)	Lithology	Sample Location	Core Descriptions	Interpretations
7	344'			Unit 7: 346' 6" to 340' 6" 106.3 to 103.8 m Silt–shale interlaminations. Small bivalves concentrated in layers, occasional large plant fragments, nodules and burrows. Gradational lower contact.	
6	346' 348'			Unit 6: 348' 6" to 346' 6" 106.2 to 106.3 Shale, non–calcareous. Abundant burrows and small calcareous laminations. Plant fragments abundant. Gradational lower contact.	
5	350' 352' 354' 356'			Unit 5: 364' 6" to 348' 6" 111.1 to 106.2 m Shale, slighlty calcareous. Brachiopods rare, absent after 354', large plant fragments (>2") abundant. Scattered nodules and halos. Gradational lower contact.	

Core: K.G.S. Olson   Interval: 343' to 328', 104.5 to 99.9 m

Unit Number	Depth (ft)	Lithology	Sample Location	Core Descriptions	Interpretations
9	330' 332'	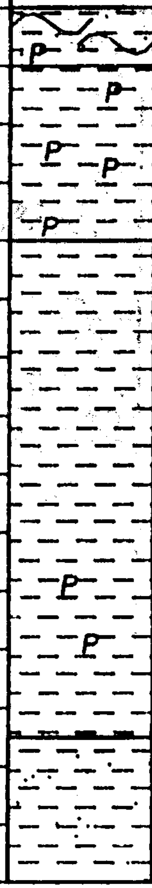		Unit 9: 332' 0" to 327' 0" 101.2 to 99.7 m Grey shale with thin silt interlaminations and flaser beds. Occasional calcareous layers, large plant fragments common. Gradational lower contact.	
8	334' 336' 338' 340'			Unit 8: 340' 6" to 332' 0" 103.8 to 101.2 m Shale, abundant calcareous lenses, laminations and brown zones. Large plant fragments present below 338'. Gradational lower contact.	
7	342'				

Core: K.G.S. Olson Interval: 328' to 313', 99.9 to 95.4 m

Unit Number	Depth (ft)	Lithology	Sample Location	Core Descriptions	Interpretations
12	314' 316' 318'	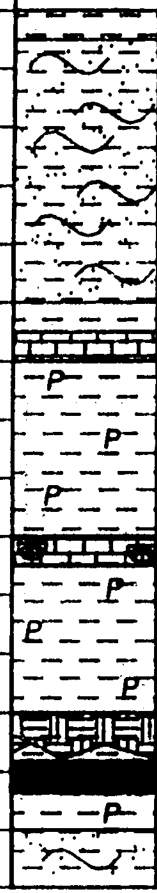	0 313'8" 0 317'3"	Unit 12: 318' 0" to 313' 3" 97.1 to 95.5 m Fine sandstone/siltstone and shale interlaminations. Sand-stone lenses may me several inches thick and have cross-beds, calcareous. Shale beds are mica rich, non-calcareous. Abrupt lower contact.	Laminations may be flaser beds, climbing ripples or starved ripples.
11	320' 322' 324'		0 318'9"	Unit 11: 325' 0" to 318' 6" 99.1 to 97.1 m Grey shale, large plant fragments common. Polished surfaces and thin carbonate layers common. Brown zones present. Brachiopods in lower carbonate zone. Grad. lower contact.	Polished areas may be peds or caused by drilling.
10	326'			Unit 10: 327' 0" to 325' 0" 99.7 to 99.1 m Grey shale, large plant debris common. Coaly interval present, contains carbonate stringers and is overlain by brown mottled zone mixed with unaltered shale layers. Gradational lower contact.	Brown mottling and large plant fragment may mark exposure surface.
9					

Core: K.G.S. Olson Interval: 315' to 308', 96.6 to 93.9 m

Unit Number	Depth (ft)	Lithology	Sample Location	Core Descriptions	Interpretations
15	306' 308' 310'	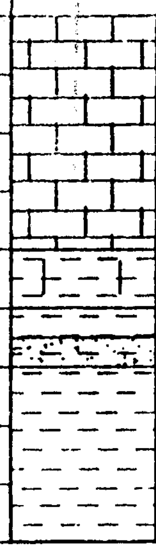		Unit 15: 310' 0" to 292' 6" 94.5 to 89.2 m Fossil rich limestone. Abrupt lower contact.	Mound Valley limestone.
14				Unit 14: 310' 6" to 310' 0" 94.6 to 94.5 m Fossiliferous calcareous shale. Brachiopods, crinoid fragments and bryozoans common. Increasingly calcareous upwards. Grad. lower contact.	
13	312' 314'			Unit 13: 313' to 310' 6" 95.5 to 94.6 m Grey shale, calcareous siltstone laminations and halos common. Occasional cross-lamination in siltstone beds. Grad. lower contact.	

Core: O.G.S. Hardin Interval: 211' to 196', 59.7 to 64.0 m

Unit Number	Depth (ft)	Lithology	Sample Location	Core Descriptions	Interpretations
2	198' 200' 202' 204'	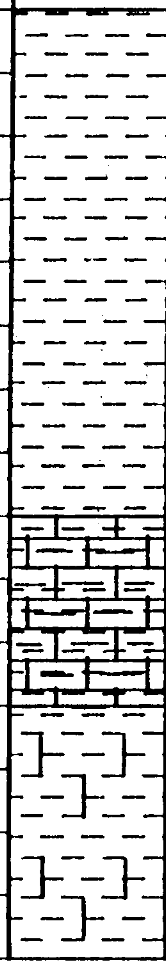		Unit 2: 190' 0" to 203' 10" 57.9 to 62.1 m Silty shale. Occasional nodules, rare silt laminations and brachiopods in lower part of unit. Gradational lower contact.	Lowest Ladore shale.
1	206' 208' 210'			Unit 1: < 203' 10" < 62.1 m Crinoidal arg. limestone grading downwards into calcareous shale.	Bethany Falls limestone.

Core: O.G.S. Hardin

Interval: 181' to 168', 55.2 to 59.7 m

Unit Number	Depth (ft)	Lithology	Sample Location	Core Descriptions	Interpretations
3	182' 184' 186' 188' 190'	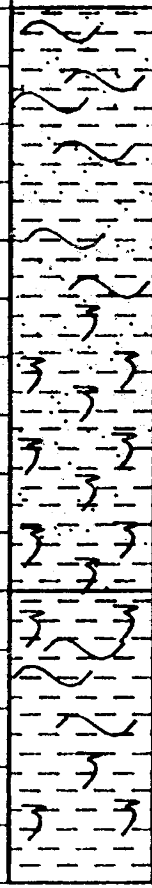		Unit 3: 179' 6" to 190' 0" 54.7 to 57.9 m Silty shale with siltstone interlaminations, decreasing in abundance downwards. Starved ripples, flasers, load structures, common, decreasing downwards. Burrows increasing downwards. Gradational lower contact.	
2	192' 194'				

Core: O.G.S. Hardin Interval: 168' to 183', 51.2 to 55.2 m

Unit Number	Depth (ft)	Lithology	Sample Location	Core Descriptions	Interpretations
4	170' 172' 174' 176' 178'	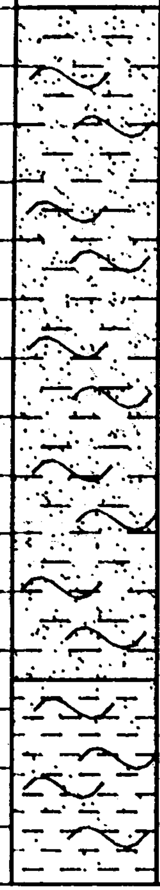	Ha 169'8" Ha 171'0"*	Unit 4: 167' 8" to 179' 6" 51.1 to 54.7 m Siltstone and shale interlaminations, starved ripples and flaser bed. Silt lenses show cross-bedding. Thickness of silt lenses decreases downwards. Abrupt lower contact.	
3	180' 182'				

Core: O.G.S. Hardin   Interval: 153' to 168', 46.6 to 51.2 m

Unit Number	Depth (ft)	Lithology	Sample Location	Core Descriptions	Interpretations
9	154'			Unit 9: 153' 2" to 153' 10" 46.5 to 46.9 m Sandstone, massive bedding. Abundant large plant fragments Nodules increasing downward. Sharp lower contact.	
8	156' 158'		Ha 155'6"s Ha 155'9"s	Unit 8: 153' 10" to 159' 2" 46.9 to 48.5 m Sandstone and shale interlam. with frequent cross-bedding. Flaser beds and convluted beds rare. Plant fragments rare. Sharp lower contact.	
7	160' 162' 164'		Ha 163'0"	Unit 7: 159' 2" to 165' 10" 48.5 to 50.6 m Massive bedded sandstone with occasional flaser beds and thin shale laminations is upper unit. Nodules common. In base. Sharp lower contact.	Channel lag deposit.
6	166'			Unit 6: 165' 10 to 167' 0" 50.6 to 50.9 m Shale with interlaminations of siltstone and sandstone. Lenticular sand beds show cross lamination and starved ripples. Mica abundant in shale. Sharp lower contact.	
5				Unit 5: 167' 10" to 179' 8" 50.9 to 51.1 m Sandstone with silty shale interbeds. Shale decreasing downward. Sharp lower contact.	

[redacted]

Core: O.G.S. Hardin   Interval: 138' to 158', 42.1 to 46.6 m

Unit Number	Depth (ft)	Lithology	Sample Location	Core Descriptions	Interpretations
14	140'	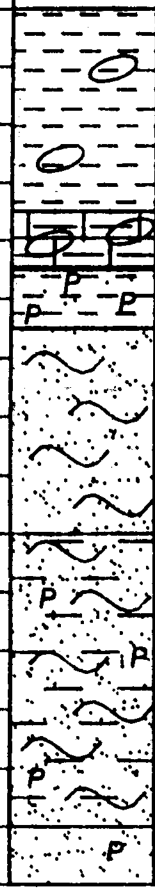		Unit 14: 141' 8"+ 43.2+ m Shale, thinly bedded nodules common. Grad. lower contact.	Galesburg shale.
13	142'			Unit 13: 141' 8" to 142' 10" 43.2 to 43.5 m Arg. limestone. Crinoid and brachiopod debris common. Nodules present. Abr. lower con.	Mound Valley limestone.
12				Unit 12: 142' 10" to 143' 5" 43.5 to 43.7 m Interlaminated siltstone and shale. Single and continuous beds showing some cross lamination. Small plant fragments common. Sharp lower contact.	Top of Ladore shale.
11	144' 146'		Ha 145'6" Ha 145'11"s Ha 146'0"	Unit 11: 143' 5" to 147' 0" 43.7 to 44.8 m Fine sandstone with frequent flaser beds, increasing down. Herringbone cross-beds present. Sharp lower contact.	
10	148' 150'		Ha 148'5"s	Unit 10: 143' 5" to 152' 5" 44.8 to 46.5 m Sandstone/shale inter-lam., containing multidirectional cross laminations. Starved ripples and small plant common. Gradational lower contact.	
9	152'		Ha 152'11"		

APPENDIX B:
POINT COUNT DATA

	O.G.S. Hardin:							
	Ha 145'6"		Ha 145' 11" s		Ha 146'0"		Ha 148' 5" s	
Mineral	#	%	#	%	#	%	#	%
Monocryst. Quartz	112	44.8	133	53.2	126	50.4	163	65.2
Polycryst. Quartz	6	2.4	6	2.4	5	2	3	1.2
Orthoclase	14	5.6	9	3.6	4	1.6	17	6.8
Plagioclase	1	0.4	6	2.4	3	1.2	5	2
Muscovite	11	4.4	11	4.4	10	4	23	9.2
Biotite	TR	0	2	0.8	1	0.4	1	0.4
Chert	4	1.6	4	1.6	0	0	3	1.2
Calcite Cement	37	14.8	33	13.2	59	23.6	2	0.8
Pyrite	0	0	1	0.4	0	0	0	0
Iron Oxide	1	0.4	1	0.4	0	0	4	1.6
Kaolinite	15	6	13	5.2	12	4.8	10	4
Chlorite	20	8	7	2.8	2	0.8	11	4.4
Illite	0	0	2	0.8	11	4.4	0	0
Primary Porosity	0	0	2	0.8	2	0.8	1	0.4
Secondary Porosity	3	1.2	4	1.6	12	4.8	3	1.2
Metamorphic Rx. Frag.	6	2.4	2	0.8	3	1.2	0	0
Sedimentary Rx. Frag.	0	0	0	0	0	0	0	0
Siderite	0	0	0	0	0	0	0	0
Microcline	1	0.4	0	0	0	0	0	0
Zircon	1	0.4	2	0.8	TR	0	2	0.8
Tourmaline	0	0	0	0	0	0	0	0
Garnet	0	0	2	0.8	0	0	0	0
Organics	12	4.8	10	4	0	0	2	0.8
Box-work Fe oxide	0	0	0	0	0	0	0	0
Rutile	TR	0	0	0	TR	0	0	0
Quartz Overgrowths	TR	0	0	0	0	0	0	0
Siltstone Frag.	6	0	0	0	0	0	0	0
Fossil Fragments	0	0	0	0	0	0	0	0
n=	250		250		250		250	
% Quartz	81.94		86.88		92.91		86.91	
% Feldspars	11.11		9.38		4.96		11.52	
% Rock Fragments	6.94		3.75		2.13		1.57	
% Total	100.00		100.00		100.00		100.00	

	Ha 152'11"		Ha 155' 6" s		Ha 159'6"		Ha 155' 9" s	
Mineral	#	%	#	%	#	%	#	%
Monocryst. Quartz	118	47.2	101	40.4	110	44	110	44
Polycryst. Quartz	3	1.2	6	2.4	8	3.2	4	1.6
Orthoclase	7	2.8	28	11.2	11	4.4	15	6
Plagioclase	3	1.2	6	2.4	10	4	7	2.8
Muscovite	23	9.2	13	5.2	6	2.4	20	8
Biotite	0	0	0	0	0	0	2	0.8
Chert	4	1.6	5	2	4	1.6	5	2
Calcite Cement	24	9.6	29	11.6	19	7.6	0	0
Pyrite	0	0	5	2	10	4	0	0
Iron Oxide	0	0	10	4	0	0	5	2
Kaolinite	19	7.6	7	2.8	19	7.6	6	2.4
Chlorite	7	2.8	4	1.6	5	2	4	1.6
Illite	5	2	0	0	0	0	5	2
Primary Porosity	3	1.2	0	0	10	4	0	0
Secondary Porosity	7	2.8	7	2.8	36	14.4	0	0
Metamorphic Rx. Frag.	3	1.2	7	2.8	2	0.8	1	0.4
Sedimentary Rx. Frag.	0	0	0	0	0	0	55	22
Siderite	0	0	0	0	0	0	0	0
Microcline	0	0	0	0	0	0	0	0
Zircon	0	0	0	0	0	0	1	0.4
Tourmaline	0	0	0	0	0	0	0	0
Garnet	0	0	0	0	0	0	0	0
Organics	15	6	22	8.8	0	0	6	2.4
Box-work Fe oxide	0	0	0	0	0	0	0	0
Rutile	0	0	0	0	0	0	0	0
Quartz Overgrowths	0	0	0	0	0	0	0	0
Siltstone Frag.	9	3.6	0	0	0	0	0	0
Fossil Fragments	0	0	0	0	0	0	0	0
n=	250		250		250		246	
% Quartz	87.68		69.93		81.38		57.87	
% Feldspars	7.25		22.22		14.48		11.17	
% Rock Fragments	5.07		7.84		4.14		30.96	
% Total	100.00		100.00		100.00		100.00	

	Ha 163'0"		Ha 165'9"		Ha 169'8"		Ha 171' 0" s	
Mineral	#	%	#	%	#	%	#	%
Monocryst. Quartz	131	52.4	118	47.2	131	52.4	117	46.8
Polycryst. Quartz	9	3.6	5	2	7	2.8	4	1.6
Orthoclase	20	8	19	7.6	13	5.2	21	8.4
Plagioclase	8	3.2	5	2	6	2.4	5	2
Muscovite	8	3.2	9	3.6	14	5.6	23	9.2
Biotite	0	0	2	0.8	1	0.4	5	2
Chert	6	2.4	4	1.6	5	2	3	1.2
Calcite Cement	17	6.8	26	10.4	19	7.6	9	3.6
Pyrite	0	0	0	0	0	0	0	0
Iron Oxide	0	0	2	0.8	3	1.2	16	6.4
Kaolinite	5	2	9	3.6	16	6.4	14	5.6
Chlorite	0	0	13	5.2	13	5.2	8	3.2
Illite	1	0.4	3	1.2	2	0.8	2	0.8
Primary Porosity	8	3.2	4	1.6	3	1.2	0	0
Secondary Porosity	26	10.4	26	10.4	14	5.6	0	0
Metamorphic Rx. Frag.	8	3.2	3	1.2	3	1.2	3	1.2
Sedimentary Rx. Frag.	1	0.4	0	0	0	0	0	0
Siderite	0	0	0	0	0	0	0	0
Microcline	0	0	0	0	0	0	0	0
Zircon	0	0	1	0.4	TR	0	3	1.2
Tourmaline	1	0.4	TR	0	0	0	0	0
Garnet	0	0	0	0	0	0	0	0
Organics	1	0.4	1	0.4	0	0	17	6.8
Box-work Fe oxide	0	0	0	0	0	0	0	0
Rutile	0	0	0	0	0	0	0	0
Quartz Overgrowths	0	0	0	0	0	0	0	0
Siltstone Frag.	0	0	0	0	0	0	0	0
Fossil Fragments	0	0	0	0	0	0	0	0
n=	250		250		250		250	
% Quartz	76.50		79.87		83.64		79.08	
% Feldspars	15.30		15.58		11.52		16.99	
% Rock Fragments	8.20		4.55		4.85		3.92	
% Total	100.00		100.00		100.00		100.00	

	K.G.S. Olson						K.G.S. Kinne	
	O 313' 8"		O 317' 3"		O 318' 9"		Ki 105' 4"	
Mineral	#	%	#	%	#	%	#	%
Monocryst. Quartz	121	48.4	101	40.4	72	28.8	94	37.6
Polycryst. Quartz	0	0	0	0	1	0.4	0	0
Orthoclase	4	1.6	2	0.8	3	1.2	1	0.4
Plagioclase	4	1.6	2	0.8	3	1.2	1	0.4
Muscovite	7	2.8	20	8	4	1.6	72	28.8
Biotite	3	1.2	0	0	0	0	0	0
Chert	0	0	0	0	0	0	0	0
Calcite Cement	76	30.4	109	43.6	56	22.4	39	15.6
Pyrite	4	1.6	0	0	0	0	1	0.4
Iron Oxide	0	0	0	0	0	0	2	0.8
Kaolinite	6	2.4	12	4.8	61	24.4	28	11.2
Chlorite	2	0.8	2	0.8	3	1.2	1	0.4
Illite	0	0	0	0	0	0	0	0
Primary Porosity	0	0	0	0	0	0	0	0
Secondary Porosity	0	0	0	0	0	0	0	0
Metamorphic Rx. Frag.	0	0	0	0	0	0	0	0
Sedimentary Rx. Frag.	0	0	0	0	0	0	0	0
Siderite	0	0	0	0	0	0	3	1.2
Microcline	0	0	0	0	0	0	0	0
Zircon	TR	0	1	0.4	0	0	TR	0
Tourmaline	0	0	0	0	0	0	0	0
Garnet	0	0	0	0	0	0	0	0
Organics	3	1.2	1	0.4	1	0.4	6	2.4
Box-work Fe oxide	0	0	0	0	0	0	0	0
Rutile	0	0	0	0	0	0	0	0
Quartz Overgrowths	0	0	0	0	0	0	0	0
Siltstone Frag.	0	0	0	0	0	0	0	0
Fossil Fragments	20	8	TR	0	46	18.4	2	0.8
n=	250		250		250		250	
% Quartz	93.80		96.19		92.41		97.92	
% Feldspars	6.20		3.81		7.59		2.08	
% Rock Fragments	0.00		0.00		0.00		0.00	
% Total	100		100		100		100	

	K.G.S. Gaddy					
	G 314' 2"		G 315' 4"		G 315' 4" s	
Mineral	#	%	#	%	#	%
Monocryst. Quartz	101	40.4	112	44.8	114	45.6
Polycryst. Quartz	0	0	1	0.4	7	2.8
Orthoclase	2	0.8	3	1.2	15	6
Plagioclase	2	0.8	3	1.2	2	0.8
Muscovite	22	8.8	28	11.2	22	8.8
Biotite	0	0	1	0.4	5	2
Chert	0	0	0	0	0	0
Calcite Cement	106	42.4	88	35.2	63	25.2
Pyrite	0	0	0	0	1	0.4
Iron Oxide	0	0	0	0	0	0
Kaolinite	12	4.8	10	4	12	4.8
Chlorite	2	0.8	3	1.2	4	1.6
Illite	0	0	0	0	0	0
Primary Porosity	0	0	0	0	0	0
Secondary Porosity	0	0	0	0	0	0
Metamorphic Rx. Frag.	0	0	0	0	0	0
Sedimentary Rx. Frag.	0	0	0	0	0	0
Siderite	0	0	0	0	0	0
Microcline	0	0	0	0	0	0
Zircon	1	0.4	0	0	0	0
Tourmaline	0	0	0	0	0	0
Garnet	0	0	0	0	0	0
Organics	1	0.4	1	0.4	5	2
Box-work Fe oxide	0	0	0	0	0	0
Rutile	0	0	0	0	0	0
Quartz Overgrowths	0	0	0	0	0	0
Siltstone Frag.	0	0	0	0	0	0
Fossil Fragments	1	0.4	0	0	0	0
n=	250		250		250	
% Quartz	96.19		94.96		87.68	
% Feldspars	3.81		5.04		12.32	
% Rock Fragments	0.00		0.00		0.00	
% Total	100.00		100.00		100.00	

	G 316' 4"		G 316' 8"		G 317' 3" s	
Mineral	#	%	#	%	#	%
Monocryst. Quartz	70	28	88	35.2	63	25.2
Polycryst. Quartz	0	0	0	0	1	0.4
Orthoclase	1	0.4	3	1.2	4	1.6
Plagioclase	2	0.8	3	1.2	1	0.4
Muscovite	11	4.4	2	0.8	38	15.2
Biotite	1	0.4	0	0	3	1.2
Chert	0	0	0	0	1	0.4
Calcite Cement	141	56.4	138	55.2	110	44
Pyrite	2	0.8	0	0	1	0.4
Iron Oxide	0	0	1	0.4	3	1.2
Kaolinite	4	1.6	0	0	7	2.8
Chlorite	5	2	9	3.6	1	0.4
Illite	0	0	0	0	0	0
Primary Porosity	0	0	0	0	0	0
Secondary Porosity	0	0	0	0	0	0
Metamorphic Rx. Frag.	0	0	0	0	1	0.4
Sedimentary Rx. Frag.	0	0	0	0	0	0
Siderite	0	0	0	0	0	0
Microcline	0	0	0	0	0	0
Zircon	TR	0	1	0.4	0	0
Tourmaline	0	0	0	0	0	0
Garnet	0	0	0	0	0	0
Organics	5	2	0	0	16	6.4
Box-work Fe oxide	0	0	0	0	0	0
Rutile	0	0	0	0	0	0
Quartz Overgrowths	0	0	0	0	0	0
Siltstone Frag.	0	0	0	0	0	0
Fossil Fragments	8	3.2	5	2	0	0
n=	250		250		250	
% Quartz	95.89		93.62		90.14	
% Feldspars	4.11		6.38		7.04	
% Rock Fragments	0.00		0.00		2.82	
% Total	100.00		100.00		100.00	

Lower Coffeyville Section:								
	LCS 8.0		LCS 14.5 s		LCS 14.9		LCS 15.0	
Mineral	#	%	#	%	#	%	#	%
Monocryst. Quartz	149	59.6	138	55.2	173	69.2	151	60.4
Polycryst. Quartz	6	2.4	0	0	5	2	4	1.6
Orthoclase	5	2	10	4	1	0.4	6	2.4
Plagioclase	1	0.4	1	0.4	0	0	3	1.2
Muscovite	18	7.2	31	12.4	2	0.8	10	4
Biotite	2	0.8	6	2.4	1	0.4	0	0
Chert	1	0.4	0	0	0	0	2	0.8
Calcite Cement	5	2	0	0	0	0	0	0
Pyrite	2	0.8	0	0	0	0	0	0
Iron Oxide	17	6.8	0	0	20	8	18	7.2
Kaolinite	27	10.8	0	0	9	3.6	13	5.2
Chlorite	12	4.8	38	15.2	18	7.2	16	6.4
Illite	0	0	11	4.4	0	0	0	0
Primary Porosity	2	0.8	12	4.8	3	1.2	3	1.2
Secondary Porosity	0	0	1	0.4	15	6	12	4.8
Metamorphic Rx. Frag.	0	0	1	0.4	3	1.2	9	3.6
Sedimentary Rx. Frag.	0	0	0	0	0	0	0	0
Siderite	0	0	0	0	0	0	0	0
Microcline	1	0.4	0	0	0	0	0	0
Zircon	0	0	1	0.4	0	0	1	0.4
Tourmaline	0	0	0	0	0	0	1	0.4
Garnet	1	0.4	0	0	0	0	0	0
Organics	1	0.4	0	0	0	0	1	0.4
Box-work Fe oxide	0	0	0	0	0	0	0	0
Rutile	0	TR	0	0	0	0	0	0
Quartz Overgrowths	0	TR	0	TR	0	0	0	0
Siltstone Frag.	0	0	0	0	0	0	0	0
Fossil Fragments	0	0	0	0	0	0	0	0
n=	250		250		250		250	
% Quartz	95.09		92.00		97.80		88.57	
% Feldspars	4.29		7.33		0.55		5.14	
% Rock Fragments	0.61		0.67		1.65		6.29	
% Total	100.0		100.0		100.0		100.0	

			Dixon Mound		Parson's Lake	
	LCS 16.0		DM 1.0		PL 5.2	
Mineral	#	%	#	%	#	%
Monocystalline Quartz	153	61.2	77	30.8	89	35.6
Polycrystalline Quartz	9	3.6	1	0.4	1	0.4
Orthoclase	8	3.2	7	2.8	0	0
Plagioclase	2	0.8	2	0.8	0	0
Muscovite	1	0.4	32	12.8	12	4.8
Biotite	0	0	2	0.8	0	0
Chert	1	0.4	0	0	2	0.8
Calcite Cement	0	0	3	1.2	83	33.2
Pyrite	0	0	0	0	1	0.4
Iron Oxide	17	6.8	0	0	5	2
Kaolinite	3	1.2	113	45.2	37	14.8
Chlorite	4	1.6	1	0.4	10	4
Illite	0	0	0	0	0	0
Primary Porosity	7	2.8	0	0	0	0
Secondary Porosity	22	8.8	0	0	0	0
Metamorphic Rx. Frag.	3	1.2	0	0	0	0
Sedimentary Rx. Frag.	0	0	0	0	0	0
Siderite	0	0	0	0	0	0
Microcline	1	0.4	0	0	0	0
Zircon	0	0	0	0	1	0.4
Tourmaline	0	0	0	0	0	0
Garnet	0	0	0	0	0	0
Organics	0	0	12	4.8	9	3.6
Box-work Fe oxide	19	7.6	0	0	0	0
Rutile	0	0	0	0	0	0
Quartz Overgrowths	0	0	0	0	0	0
Siltstone Frag.	0	0	0	0	0	0
Fossil Fragments	0	0	0	0	0	0
n=	250		250		250	
% Quartz	91.53		89.66		97.83	
% Feldspars	6.21		10.34		0.00	
% Rock Fragments	2.26		0.00		2.17	
% Total	100.0		100.0		100.0	